Petroleum Science and Engineering
2024, Vol. 8, No. 2, pp. 70-99
https://doi.org/10.11648/j.pse.20240802.12

Research Article

Simplified Neural Network-Based Models for Oil Flow Rate Prediction

Uduak Koffi Umana, Anietie Ndarake Okon, Okorie Ekwe Agwu*

Department of Petroleum Engineering, University of Uyo, Uyo, Nigeria

Abstract

Available neural network-based models for predicting the oil flow rate (q_o) in the Niger Delta are not simplified and are developed from limited data sources. The reproducibility of these models is not feasible as the models' details are not published. This study developed simplified and reproducible three, five, and six-input variables neural-based models for estimating q_o using 283 datasets from 21 wells across fields in the Niger Delta. The neural-based models were developed using maximum-minimum (max.-min.) normalized and clip-normalized datasets. The performances and the generalizability of the developed models with published datasets were determined using some statistical indices: coefficient of determination (R^2), mean square error (MSE), root mean square error (RMSE), average relative error (ARE) and average absolute relative error (AARE). The results indicate that the 3-input-based neural models had overall R^2, MSE, and RMSE values of 0.9689, 9.6185×10^{-4} and 0.0310, respectively, for the max.-min. normalizing method and R^2 of 0.9663, MSE of 5.7986×10^{-3} and RMSE of 0.0762 for the clip scaling approach. The 5-input-based models resulted in R^2 of 0.9865, MSE of 5.7790×10^{-4} and RMSE of 0.0240 for the max.-min. scaling method and R^2 of 0.9720, MSE of 3.7243×10^{-3} and RMSE of 0.0610 for the clip scaling approach. Also, the 6-input-based models had R^2 of 0.9809, MSE of 8.7520×10^{-4} and RMSE of 0.0296 for the max.-min. normalizing approach and R^2 of 0.9791, MSE of 3.8859×10^{-3} and RMSE of 0.0623 for the clip scaling method. Furthermore, the generality performance of the simplified neural-based models resulted in R^2, RMSE, ARE, and AAPRE of 0.9644, 205.78, 0.0248, and 0.1275, respectively, for the 3-input-based neural model and R^2 of 0.9264, RMSE of 2089.93, ARE of 0.1656 and AARE of 0.2267 for the 6-input-based neural model. The neural-based models predicted q_o were more comparable to the test datasets than some existing correlations, as the predicted q_o result was the lowest error indices. Besides, the overall relative importance of the neural-based models' input variables on q_o prediction is $S > GLR > P_{wh} > T/T_{sc} > \gamma_o > BS\&W > \gamma_g$. The simplified neural-based models performed better than some empirical correlations from the assessment indicators. Therefore, the models should apply as tools for oil flow rate prediction in the Niger Delta fields, as the necessary details to implement the models are made visible.

Keywords

Neural Network, Normalization Methods, Simplified Neural-Based Models, Oil Flow Rate, Niger Delta

*Corresponding author: okorie.agwu@utp.edu.my (Okorie Ekwe Agwu)

Received: 2 August 2024; **Accepted:** 9 September 2024; **Published:** 23 September 2024

1. Introduction

The oil and gas production system has several distinct but interconnected components. These components include a porous medium that accumulates the oil or gas or both, a conduit(s)/well(s) intentionally drilled in the vertical or deviated configuration through the porous medium, a casing to stabilize the well(s), a tubing through which the fluids pass to the surface, a choke to regulate the flow of these fluids, a surface line and a separator to separate the reservoir contents into different phases based on their densities. One factor that links and is common to all the enumerated components is the fluid flow in the flowlines. If the field is subsea, that is, offshore, the flowline links with the inlet separator via a riser [1]. If a typical oil and gas production system is unpacked, Figure 1 depicts the interaction interfaces of the system.

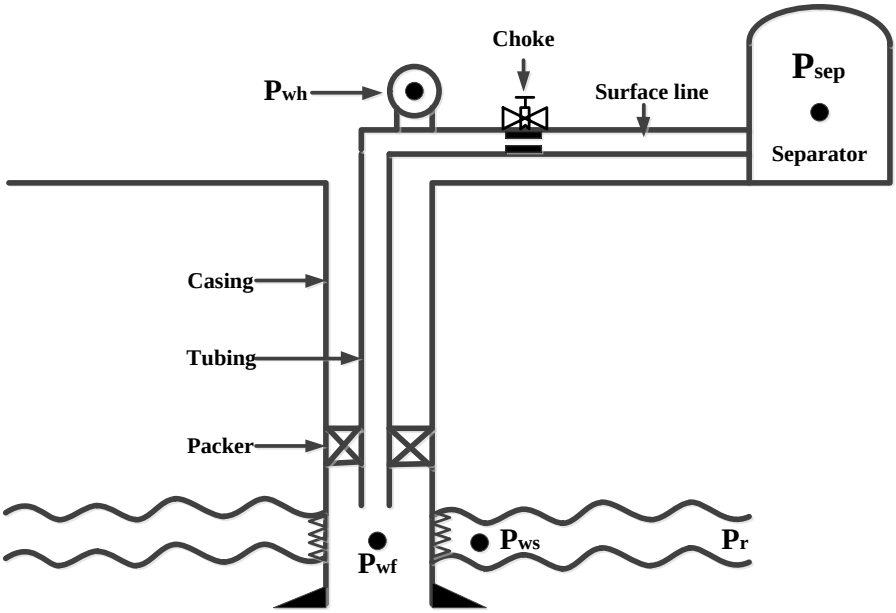

Figure 1. *A simple representation of oil and gas production system [2].*

Oil and gas metering, or the measuring of fluid flow rate, is a crucial component used as a standard to judge the economic viability of oil wells [3]. Again, understanding the flow rates of gas, oil, and water from various wells enables operators to make crucial decisions regarding rate allocation, production optimization, and future performance projection [1]. Beiranvand et al. [4] submit that when oil and gas flow rate predictions are inaccurate, they may lead to challenges such as sand production, formation damage, excessive pressures at the separator, and water coning or gas cusping [5]. Crude oil measurements are done critically at two points: first, at the wellhead to allow for the separation of basic sediment and water (BS&W) and then at the custody transfer point where the crude is measured preparatory for export [6]. Therefore, accurately quantifying the flow rate of reservoir streams provides enormous hurdles to production and subsurface engineers. The issue is that the multiphase flow meters do not present reliable production rate calculations for any fiscal purposes [3]. Then, one would ask what is challenging in detecting multiphase fluid flow rates in the field. First, the equation for multiphase flow is complex because the choke throat's changing pressure, temperature, gas-liquid ratio, and other fluid variables affect the fluid's properties. Second, multiphase flow is highly challenging because of these fluids' vastly varying densities and viscosities [7].

Fluid flow through chokes may be critical or sub-critical [8]. According to Nasriani and Kalantari [9], when the fluid approaches sonic velocity, the difference between downstream and upstream pressures is less than 0.588, and critical flow occurs in the system. The mass flow rate in this flow is determined by the pressure upstream of the bottleneck - choke. Hong and Griston [10] reported that the flow conditions are typically present in producing oil and gas wells and are also favoured for some reservoir flooding-enhanced oil recovery methods [11]. Choubineh et al. [12] maintained that critical-flow conditions are selected to achieve steady flow rates and prevent frequent changes in equipment performance for wellhead chokes.

On the other hand, when the mass flow of the fluid is lower than the sonic velocity, sub-critical flow conditions develop [4]. For the flow conditions, the mass flow rate depends on the pressure drop across any obstructions or restrictions (such as chokes) in the stream. Therefore, variations in the conditions upstream and downstream of the choke combine to affect flow rates. Thus, all the downstream-upstream pressure ratios test data less than 0.5 indicate sub-critical flow

conditions.

Numerous critical and subcritical multiphase flow correlations have been available [13]. The empirical correlations in the literature include Gilbert [14], Baxendell [15], Ros [16], Achong [17], Omana et al. [18], Pilehvari [19], Owolabi et al. [20], Al-Towailib and Al-Marhoun [21], Beiranvand et al. [4], Khorzoughi et al. [22], Okon et al. [23], Choubineh et al. [12], Ghorbani et al. [24], Alrumah and Alenezi [25], Joshua et al. [26], among others. According to Alarifi [27], the empirical correlations are distinct for particular fields or hydrocarbon types. Therefore, the application of these correlations across all oilfields is limited. On the other hand, some authors have applied the advantage of artificial intelligence (AI) or machine learning (ML) model, that is, the ability to accurately predict oil flow rates with minimal data points, to overcome the limitations of empirical correlations. So far, several works have been reported in the literature by Berneti and Shahbazian [28], Mirzaei-Paiaman and Salavati [29], Al-Khalifa and Al-Marhoun [30], Zangl et al. [31], Al-Ajmi et al. [32], Okon and Appah [33], Choubineh et al. [12], Al-Qutami et al. [34], Al-Kadem et al. [35], Khan et al. [36], Ibrahim et al. [37], Alarifi [27], etc. Regrettably, most of these presented models need to be simplified in terms of architecture to apply. Again, Alarifi [27] observed that most AI-based models are developed based on data gathered from a few wells or one field. Therefore, their validity must be improved using large datasets and various possible scenarios. These observations are problematic because the unavailability of the models' details would limit the reproducibility and validation of the models. For the Niger Delta fields, Okon and Appah [33] and Okorugbo et al. [38] have reported neural-based models' performance for predicting oil flow rate. These works are with the earlier-mentioned limitations. Therefore, it is expedient to develop simplified neural-based models(s) that are reproducible for oil flow rate prediction, keeping the stated drawbacks in mind, thus, the focus of this paper.

1.1. Overview of Neural Network

Artificial neural networks (ANNs) are computational systems inspired by biological processes that learn and use that information to predict the outcomes of complicated systems [39]. The neurons are the neural network's fundamental building block. According to Behnoud and Hosseini [40], these neurons link to create a network that can handle complex problems. ANN has three layers: input, hidden, and output layers, and the number of input parameters determines the number of neurons in the input layer [33]. Initially, computations in ANN involved connection weights (W_{i1}, W_{i2}, W_{i3},……W_{iN}) assigned to the inputs (x_1, x_2, x_3,……x_N). The individual connection weights of the input neurons are multiplied by their respective input variables. The weighted sum of the inputs and connection weights is combined with the threshold or bias (b_i), and the summation gives the neuron's output. The purpose of the bias is to change the input to the activation function by either increasing it or decreasing it [3]. The output is computed and sent to another neuron through a transfer or activation function. It is good practice to use the sigmoid transfer function for the hidden layer and the linear activation function (*purelin*) for the output layer [41]. A typical architecture that depicts the flow processes in a neural network is visible in Figure 2.

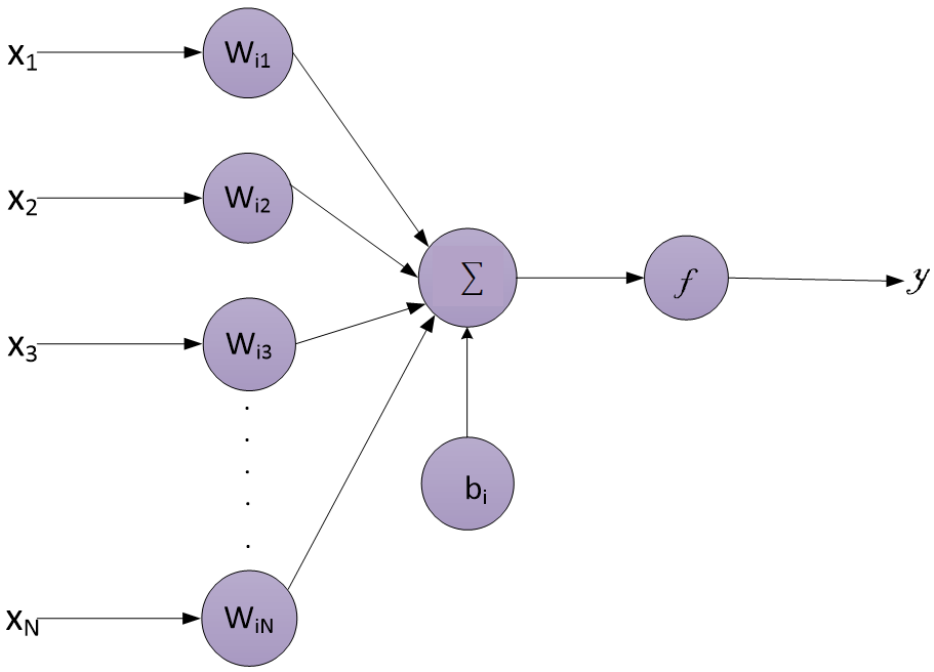

Figure 2. *A typical ANN architecture [45, 46].*

The network training is the beginning of modelling with ANN. Data are processed from the input layer through the hidden layer(s) and finally to the output layer. The predicted datasets and the actual data relate in the output layer. The difference between these datasets is fed back into the model, which updates the weights between each connection (or node) and the biases of each layer. This process is known as an epoch. In this manner, training will continue for the entire dataset until the average error (mean square error, MSE) is reduced to a predefined limit [42]. The number of neurons in the hidden layer affects network performance as fewer neurons lead to under-fitting, while too many neurons result in over-fitting. Therefore, optimizing the design of neurons is necessary [43, 44]. The several sorts of ANN include Feed-forward back-propagation neural networks (FFBP), Modular neural networks, Radial basis function (RBF), Recurrent neural networks (RNN), Convolution neural networks (CNN), Multilayer Perceptron (MLP), Deep neural network (DNN), among others.

1.2. Overview of Some Existing Neural Network Models for Oil Flow Rate Prediction

Correlations to estimate flow rate from the wellhead or through choke have received attention in the literature. Several empirical correlations have been developed for critical and subcritical flow conditions [27, 47]. For the critical flow condition, Gilbert [14] presented pioneering work using wellhead pressure (P_{wh}), choke (bean) size (S) and gas-liquid ratio (GLR) [48]. Afterward, other authors like Baxendell [15], Ros [16], Achong [17] and [19] updated Gilbert's [14] correlation constants. Also, Beiranvand et al. [4], Khorzoughi et al. [22], and Choubineh et al. [12] modified Gilbert's correlation to include basic sediments and water (BS&W), well-flowing temperature (T), oil gravity (γ_o) and gas gravity (γ_g) for liquid flow rate estimation. According to Alarifi [27], empirical correlation accuracy is very low compared to the actual field flow rate datasets. This observation is because of the assumptions applied to developing these correlations. Also, Agwu et al. [3] criticized the flexibility and replicability of these correlations and then supported the use of artificial intelligence (AI) models for flow rate prediction. A comprehensive review of the AI-based models for liquid flow rate prediction is visible in Barjouei et al. [49] and Agwu et al. [3]. An extract of the neural network and its variant models for flow rate prediction is in Table 1. The table indicates that most available ANN models for flow rate prediction are developed using datasets from the Iran oilfields. Regrettably, some of these models are not applicable as their structures are too complex for incorporation into computer programs (software). Earlier, Okon et al. [23] opined that the performance of these models is limited by the quantity and data source upon which the models are developed. Again, Table 1 further revealed that Okon and Appah [33] and Okorugbo et al. [38] works are the only available neural-based model for predicting the oil flow rate in the Niger Delta region. Unfortunately, reproducing these models is doubtful, as the authors did not publish the models' details: training algorithm, transfer (activation) functions, weights and biases. Therefore, their implementation in any petroleum engineering package is limited or not visible. Hence, the need to develop simplified neural-based models for oil flow rate prediction in the Niger Delta is necessary.

Table 1. *Some existing works on artificial neural networks and their hybrids for oil flow rate prediction.*

#	Author(s)	Datasets Source / Points	Artificial Intelligence Approach	Input Variables	Output Variable	Model Performance	Model / Architecture Pitfall
1	Berneti and Shahbazian [28]	Source: Iran Oilfield Datasets: 31 oil wells	ANN and ICA Architecture: 2-7-1	P_{wh}, T	q_o	MSE = 0.0123 RMSE = 0.1109 R^2 = 0.9703 R = 0.9850	The models' structures are simple and applicable for development.
2	Mirzaei-Paiaman and Salavati [29]	Source: Iran Oilfield Datasets: 134	ANN Architecture: 3-4-1	P_{wh}, S, GOR	q_o	AARE = 2.110 ARE = -0.330 R^2 = 0.9998 R = 0.9999	
3	Ahmadi et al. [50]	Source: Iran Oilfields Datasets: 50 oil wells; 1600	ANN Architecture: N/A ANN-ICA	P_{wh}, T	q_o	MSE = 0.0913 RMSE = 0.3022 R^2 = 0.9391 R = 0.9691 MSE = 0.0030	Models' structures are not provided to assess their simplicity and applicability.

#	Author(s)	Datasets Source / Points	Artificial Intelligence Approach	Input Variables	Output Variable	Model Performance	Model / Architecture Pitfall
			Architecture: N/A			RMSE = 0.0551 R^2 = 0.9951 R = 0.9976	
4	Al-Khalifa and Al-Marhoun [30]	Source: Middle East fields Datasets: 4031	ANN Architecture: 6-9-5-8-1	P_{wh}, T, S, GOR, γ_o, γ_g	q_L	MSE = 110.25 RMSE = 10.50 R^2 = 0.9860 R = 0.9930	The model architecture is complex and not applicable.
5	Zangl et al. [31]	Source: N/A Datasets: 258	ANN Architecture: N/A	P_{wh}, q_{gl}, P_{gl}, P_{fl}	q_o	R^2 = 0.9308 R = 0.9648	Models' structures are not provided to assess their simplicity and applicability.
6	Gorjaei et al. [51]	Source: Iran Oilfields Datasets: 276	PSO-LSSVM Architecture: N/A	S, P_{wh}, GLR	q_o	AARE = 0.70 R^2 = 0.9935 R = 0.9967	
7	Hasanvand and Berneti [52]	Source: Iran Oilfields Datasets: 600	ANN Architecture: 2-7-1	T, P_{fl}	q_{oc}	MSE = 0.0094 RMSE = 0.097 R^2 = 0.9874 R = 0.9937	The model architecture is simple and applicable for development.
8	Al-Ajmi et al. [32]	Source: N/A Datasets: 174	ANN Architecture: N/A	P_{wh}, S, T, GOR, WCT	q_L	MAPE = 15.15 R^2 = 0.890 R = 0.9434	Model architecture is not provided to assess its simplicity and application.
9	Okon and Appah [33]	Source: Niger Delta Oilfields Datasets: 64	ANN Architecture: 3-6-5-1 ANN Architecture: 5-6-6-1	P_{wh}, S, GLR P_{wh}, S, GLR, T, BS&W	q_o	AARE = 0.1920 R^2 = 0.9653 R = 0.9825 AARE = 0.1045 R^2 = 0.9951 R = 0.9976	Models' structures (two hidden layers) could be more complex.
10	Baghban et al. [53]	Source: Iran Oilfields Datasets: 100	SVM Architecture: N/A	P_{wh}, S, GOR	q_L	R^2 = 0.9998 R = 0.9999	
11	Buhulaigah et al. [54]	Source: Middle East Oilfields Datasets: 174	ANN Architecture: N/A	P_{wh}, L_e, S, P_R, k, n_L, D_{OH}	q_o	R^2 = 0.9140 R = 0.9560	Models' structures are not provided to assess their simplicity and applicability.
12	Choubineh et al. [12]	Source: Iran Oilfields Datasets: 113	ANN-TLBO Architecture: N/A	P_{wh}, S, GLR, T, γ_o, γ_g	q_{cL}	AARE = 6.50 ARE = 2.09 R^2 = 0.9810 R = 0.9905	
13	Al-Qutami et al. [34]	Source: N/A Datasets: 238	NN ensemble and ASA Architecture: N/A	T, P_{wh}, BHP, S	q_L	MAPE = 4.70 MSE = 0.0034 RMSE = 0.0585	
14	Khan et al. [55]	Source: N/A Datasets: 1500	ANN Architecture: 5-6-1	P_{wh}, S, T, γ_{API}	q_o	AARE = 2.50 R^2 = 0.9940 R = 0.9970	Models' structures have a single hidden layer that is

#	Author(s)	Datasets Source / Points	Artificial Intelligence Approach	Input Variables	Output Variable	Model Performance	Model / Architecture Pitfall
15	Al-Kadem et al. [35]	Source: N/A Datasets: 1854	ANN Architecture: 3-10-1	P_{wh}, S, GOR	q_o	AARE = 3.70 R^2 = 0.80 R = 0.8944	simple to apply.
16	Ghorbani et al. [56]	Source: Iran Oilfields Datasets: 182	GA Architecture: N/A	P_{wh}, S, GLR, BS&W	q_L	AARE = 7.33 ARE = -2.890 R^2 = 0.9970 R = 0.9985	Models' structures are not provided to assess their simplicity and applicability.
17	Khan et al. [36]	Source: Asian Oilfields Datasets: 1400	ANN Architecture: N/A	S, P_{wh}, T, γ_{API}	q_o	AARE = 2.5618 R^2 = 0.9934 R = 0.9967	
18	Al-Rumah et al. [57]	Source: Existing works Datasets: 1111	ANN Architecture: 3-39-23-1	P_{wh}, S, GLR	q_L	AARE = 0.2206 R^2 = 0.9292 R = 0.9640	Model architecture is too complex to be applicable
19	Marfo and Kporxah [58]	Source: Ghana Oilfields Datasets: 1600	ANN Architecture: 4-2-1	q_g , THP, FBHP, t	q_o	MAPE = 3.18 R^2 = 0.9966 R = 0.9983	Model architecture is simple for application.
20	Ibrahim et al. [37]	Source: Middle East Oilfields Datasets: 548 wells	SVM Architecture: N/A RF Architecture: N/A	P_{wh}, S, GOR	q_o	AAPE = 1.40 R^2 = 0.930 R = 0.9644 AAPE = 0.75 R^2 = 0.940 R = 0.9695	The AI models' structures are not visible for assessment.
21	Okorugbo et al. [38]	Source: Niger Delta Oilfields Datasets: 1595 from 7 fields	ANN Architecture: N/A ANN-PSO Architecture: N/A	P_{wh}, S, GLR, GOR, γ_o , T, T/T_{sc}, BS&W	q_o	AARE = 28.44 APE = 7.64 R^2 = 0.8774 R = 0.9367 AARE = 35.83 APE = 12.20 R^2 = 0.8318 R = 0.9120	Models' structures are not provided to assess their simplicity and applicability.
22	Alarifi [27]	Source: N/A Datasets: 1595 from 7 fields	ANN Architecture: N/A	S, P_{wh}, T, GLR, GOR, WCT	q_o	MAPE = 19.33 R^2 = 0.8649 R = 0.930	
23	Azim [59]	Source: Egypt Oilfields Datasets: 350 from 12 fields	ANN Architecture: 6-10-1	WHT, GLR, WCT, BHT, H, A_t	q_o	MSE = 0.020 RMSE = 0.1414 R^2 = 0.9630 R = 0.9813	Model architecture is a single hidden layer with less complexity for application.

*N/A = not available

2. Methods

2.1. Data Collection and Preparation

This study collected 283 datasets from 21 producing wells across different oilfields in the Niger Delta and used them to develop neural network-based models for oil flow rate prediction. The datasets include wellhead pressure (P_{wh}), bean (choke) size (S), gas-liquid ratio (GLR), oil gravity (γ_o), basic sediments and water (BS&W), well-flowing temperature (T), gas gravity (γ_g), as the input data, and oil flow rate (q_o) as the output datasets. The gathered datasets were as required for Gilbert [14], Khorzoughi et al. [22] and Choubineh et al. [12] models' parameters for the estimation of oil well flow rate. These oil flow rate models are in Equations 1 to 3;

Gilbert [14] model:

$$q = A\frac{P_{wh}S^C}{GLR^B} \tag{1}$$

Khorzoughi et al. [22] model:

$$q = A\frac{\left(P_{wh}\right)^F S^C\left(1-\frac{BS\,\&\,W}{100}\right)^D\left(T/T_{sc}\right)^E}{GLR^B} \tag{2}$$

Choubineh et al. [12] model:

$$q = A\frac{P_{wh}S^C\left(\gamma_o\right)^D\left(\gamma_g\right)^E\left(T/T_{sc}\right)^F}{GLR^B} \tag{3}$$

where A denotes the proportionality constant and the variables B to F are exponential constants of the indicated variable in the models. These datasets' statistical parameters (i.e., maximum, minimum, range, average and standard deviation values) before and after data preprocessing are in Tables 2 and 3, respectively. Two scaling approaches, namely the maximum-minimum method (in Equation 4) and clip method (in Equation 5), were used to minimize the differences (i.e., range) between the datasets. Maximum-minimum approach normalized the datasets to values between 0 and 1, while the clip method scaled the datasets to values between -1 and 1.

$$y_{scaled} = \frac{y_i - y_{\min}}{y_{\max} - y_{\min}} \tag{4}$$

$$y_{scaled} = 2\left(\frac{y_i - y_{\min}}{y_{\max} - y_{\min}}\right) - 1 \tag{5}$$

where y_{scaled} represents the scaled values for input or output parameters, y_i is the values of the not-scaled parameters, $y_{\min}$ and $y_{\max}$ denote the minimum and maximum values of the not-scaled parameters, respectively. According to Okon and Ansa [46] and Okon et al. [60], scaling the datasets for the neural network training is necessary for the following reasons: adequate adjustment of the network connecting weights for optimum prediction and reducing the sensitivity of the sigmoidal (i.e., transfer or activation) function to large datasets values.

Table 2. *Statistical description of the datasets for the development of the neural-based models before data preprocessing.*

Parameters	Maximum	Minimum	Range	Average	Std. Dev.
Wellhead Pressure, P_{wh}	3600.0	53.65	3546.35	977.136	831.215
Bean (Choke) Size, S	114.0	14.0	100.0	48.532	26.285
Gas-Liquid Ratio, GLR	32851.7	20.175	32831.5	2851.31	5205.32
Oil Gravity, γ_o	0.9433	0.643	0.3003	0.8612	0.0564
Basic Sediments and Water, $BS\,\&\,W$	0.9750	0.0005	0.9745	0.7626	0.2104
Well Flowing Temperature, T	192.0	48.0	144.0	97.627	31.606
Gas Gravity, γ_g	0.9399	0.5227	0.4172	0.7410	0.0974
Oil Flow Rate, q_o	14417.0	183.0	14234.0	2616.11	2933.33

Table 3. *Statistical description of the datasets for developing the neural-based models after data preprocessing.*

Parameters	Maximum	Minimum	Range	Average	Std. Dev.
Wellhead Pressure, P_{wh}	3300.0	95.0	3205.0	956.318	737.64
Bean (Choke) Size, S	74.0	14.0	60.0	33.753	14.815
Gas-Liquid Ratio, GLR	28597.0	29.0	28568.0	2435.81	5025.79
Oil Gravity, γ_o	0.9433	0.7339	0.2094	0.8361	0.0443
Basic Sediments and Water, $BS\&W$	0.9430	0.0005	0.9425	0.7442	0.2053
Well Flowing Temperature, T	186.0	48.0	138.0	99.747	29.736
Gas Gravity, γ_g	0.9399	0.5227	0.4172	0.7410	0.0974
Oil Flow Rate, q_o	14417.0	183.0	14234.0	2616.11	2933.33

2.2. Neural Network Models Development

The neural fitting tool (nftool) in MATLAB (Matrix Laboratory) software 2020a was used to develop the neural network for predicting oil well flow rate (q_o). The scaled datasets from Equations 4 and 5 were grouped based on Gilbert [14], Khorzoughi et al. [22] and Choubineh et al. [12] models' input requirements. That is, P_{wh}, S and GLR (3-input) for Gilbert's model, P_{wh}, S, GLR, T/T_{sc} and BS&W (5-input) for the Khorzoughi et al.'s model, and P_{wh}, S, GLR, T/T_{sc}, γ_o and γ_g (6-input) for the Choubineh et al.'s model. These scaled data (i.e., inputs and output) were imported from Microsoft Excel to the MATLAB workspace, named accordingly, and saved. Afterward, the nftool environment was active from the command window, and the data files in the workspace moved to the nftool environment for neural network development and training. The neural network training to determine the number of hidden layer neurons was a trial-and-error approach. The networks learned the input and output datasets using the Leverberg-Marquardt algorithm based on the feed-forward back-propagation (FFBP) approach. The network generates the initial weights and biases using its random number generator. Thus, the input datasets, output data, weights, biases, and neurons at the hidden layer are combined to create the network. The outcomes of the network training (70% of the datasets), validation (15% of the datasets) and testing (15% of the datasets), based on the mean square error (MSE) and correlation coefficient (R) values, determine the network performance. For more details on the networks' stopping criteria and weight adjustment, readers can obtain from published works by Mahmoudi and Mahmoudi [61], Okon et al. [62] and Okon and Ansa [46]. Figures 3 to 5 depict the different neural network architectures obtained for the various oil flow rate models. Thus, the basic settings of the trained neural networks' parameters are in Table 4. The summary of the neural network learning processes is as follows [63]:

1) read the input datasets and the expected output;
2) calculate the network output by performing weighted sums and transfer functions;
3) compare the network predictions with the expected output (target);
4) compute and update fitness (MSE) value based on the comparison;
5) repeat steps (ii) and (iii) until all training points are exhausted;
6) adjust weights appropriately to maximize fitness; and
7) repeat steps (i) to (vi) until an acceptable fitness value is established.

Thus, the stages involved in executing this study are represented in the flowchart in Figure 6.

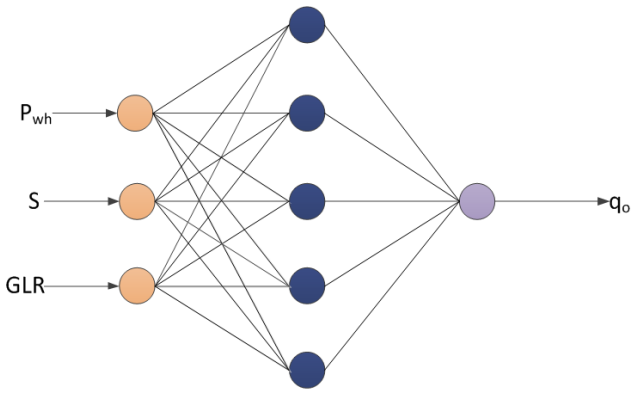

Figure 3. *Neural network architecture for a 3-input-based model.*

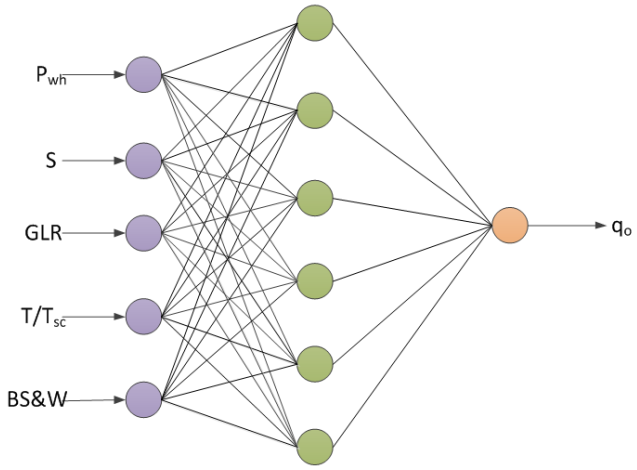

Figure 4. Neural network architecture for a 5-input-based model.

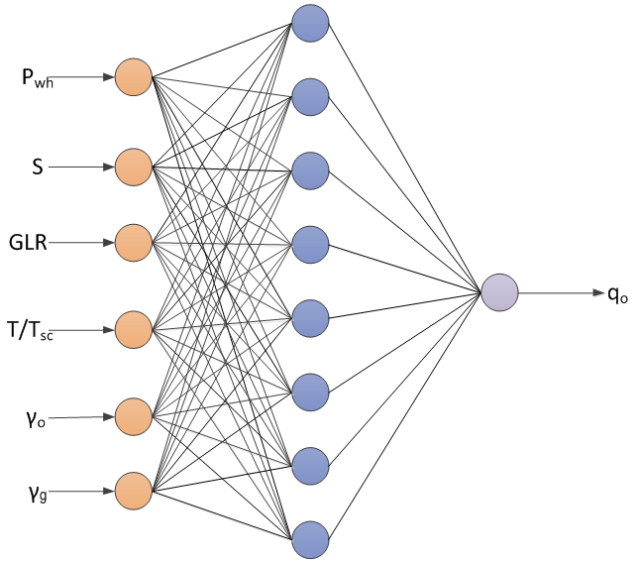

Figure 5. Neural network architecture for a 6-input-based model.

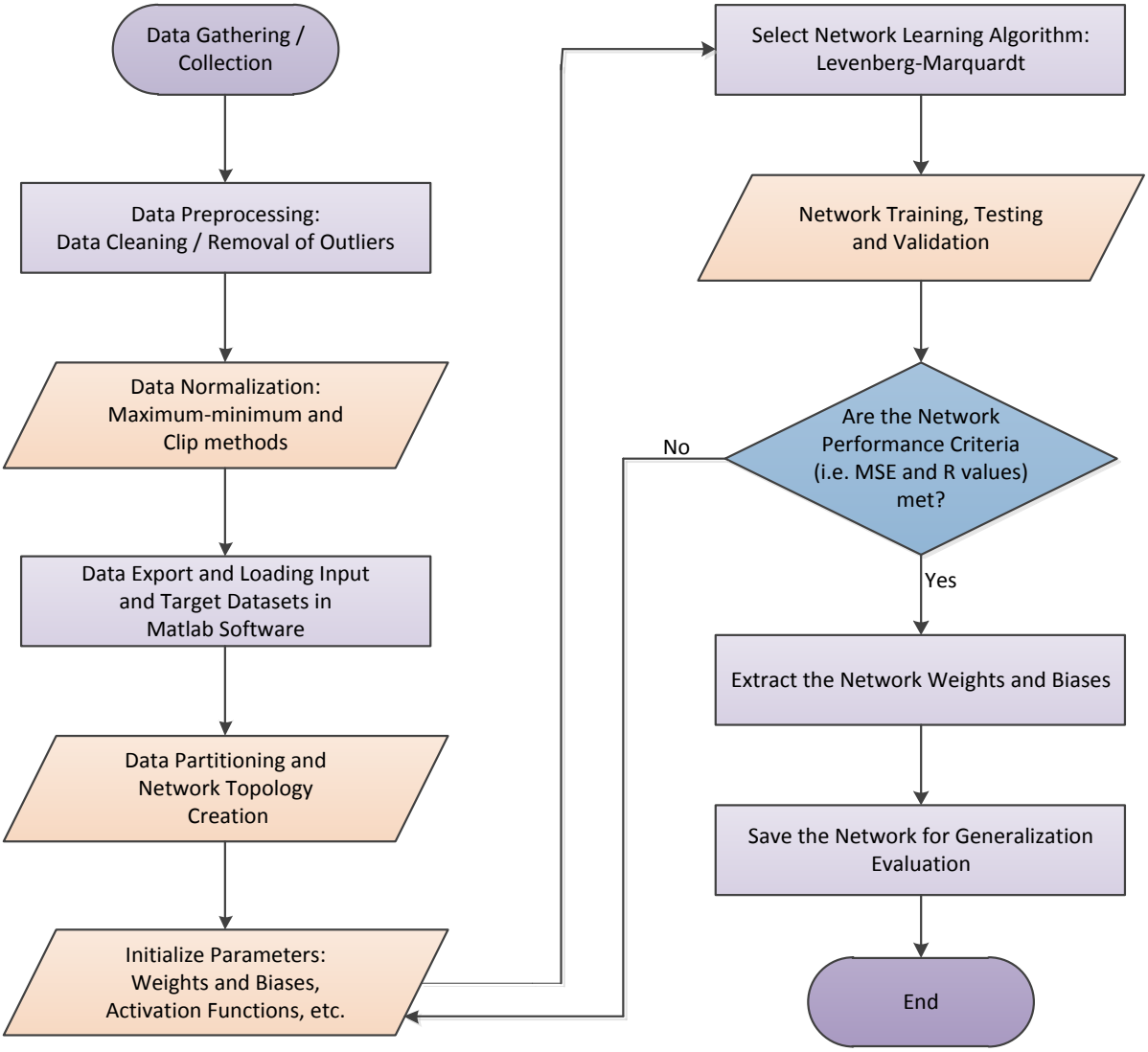

Figure 6. Flowchart of the processes involved in performing the study.

Table 4. *Basic settings of the neural networks training hyperparameters.*

Hyperparameters	Values
Training Datasets	199 (70% of the datasets)
Validation Datasets	42 (15% of the datasets)
Testing Datasets	42 (15% of the datasets)
Hidden Layer	1
Hidden Layer Neurons	5, 6, 8
Hidden Layer Activation Function	tansig
Output Layer Activation Function	purelin
Learning Algorithm	Levenberg-Marquardt
Number of Epochs	1000
Rate of Learning	0.7
Architecture Selection	Trial-and-error
Target Goal MSE	10^{-7}
Minimum Performance Gradient	10^{-7}

3. Results and Discussion

3.1. The Neural Networks Performance

The neural networks developed for oil flow rate prediction are feed-forward back-propagation networks with input, hidden, and output layers. Their architectures indicated that the best predictions were with 3-5-1 for the 3-input-based model, 5-6-1 for the 5-input-based model and 6-8-1 for the 6-input-based model. This outcome implies that the 3-input-based network has three neurons at the input layer, five at the hidden layer, and one at the output layer. The 5-input-based network has five input neurons, six hidden neurons and a neuron at the input layer. Again, the 6-input-based network has six input neurons, eight hidden neurons, and one at the output layer. Therefore, the developed networks presented in Figures 3 to 5 are multiple-inputs single-output (MISO) neural networks. Table 5 depicts the performance indices: mean square error (MSE) and coefficient of determination (R^2) values of the various networks during the training, validation and testing stages of the network development. As shown in Table 4, the 3-input-based network had overall MSE and R^2 values of 9.6185×10^{-4} and 0.9921 for the maximum-minimum normalization approach and 5.7986×10^{-3} and 0.9915 for the clip normalization method. Also, the 5-input-based network resulted in overall MSE and R^2 values of 5.7790×10^{-4} and 0.9966 for the maximum-minimum scaling approach and 3.7243×10^{-3} and 0.9929 for the clip scaling method. The 6-input-based network had overall MSE and R^2 values of 8.7523×10^{-4} and 0.9952 for the maximum-minimum data normalization method and 3.8859×10^{-3} and 0.9947 for the clip normalization approach. The network performance indices showed that the maximum-minimum normalization approach performed slightly better than the clip counterparts. This observation is because of the sigmoidal (i.e., transfer) function, which ranged between 0 and 1, as with the maximum-minimum scaling method.

Furthermore, the overall performance of the various networks showed that their predictions were close to the actual oil flow rate (q_o) data. The observation is because the MSE and R^2 values are within acceptable limits for any model/network performance. Therefore, the networks can predict the fields' q_o with a 99.0% certainty based on the R^2 values obtained. Again, the closeness of the network predicted q_o with the actual q_o datasets is visible on the diagonal trend of the output (i.e., network predictions) and target (field datasets) for the overall performance, as in Figures 7 to 9. According to Al-Bulushi et al. [64] and Okon et al. [62], when the experimental (or field) and predicted data points aligned along a unit slope, it implies a good agreement between them, as observed in Figures 7 to 9.

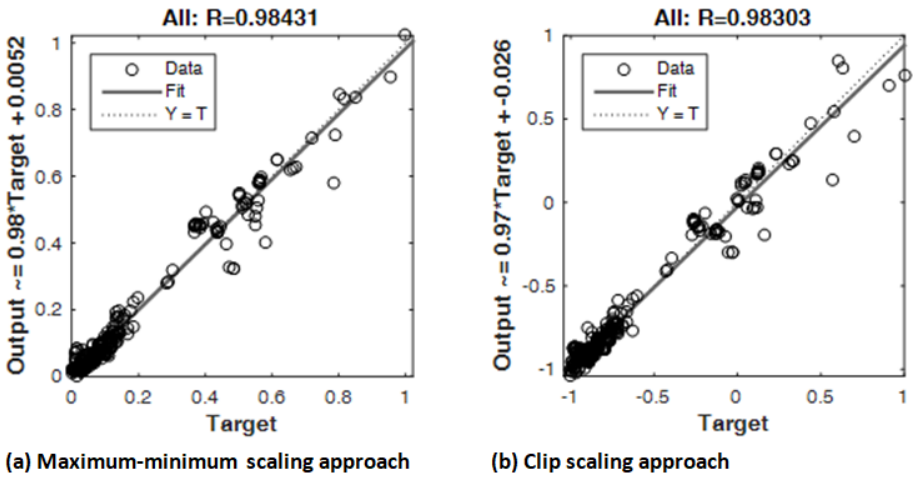

(a) Maximum-minimum scaling approach **(b) Clip scaling approach**

Figure 7. *Comparison of the normalization approaches overall performance for the 3-input-based network.*

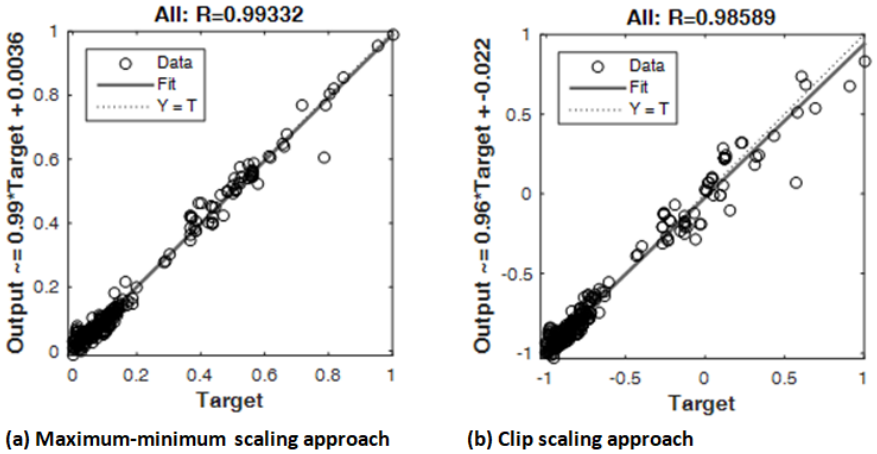

(a) Maximum-minimum scaling approach (b) Clip scaling approach

Figure 8. *Comparison of the normalization approaches overall performance for the 5-input-based network.*

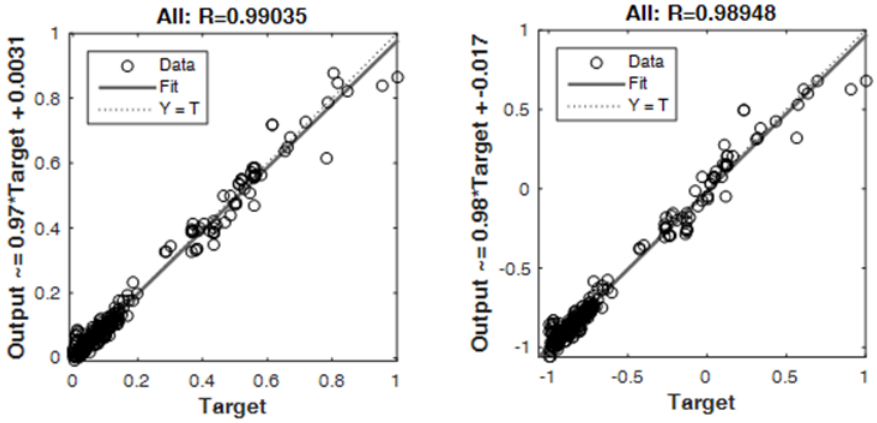

(a) Maximum-minimum scaling approach (b) Clip scaling approach

Figure 9. *Comparison of the normalization approaches overall performance for the 6-input-based network.*

Table 5. *Performance indices of the neural networks during training, validation and testing.*

	Models	Indices	Maximum-minimum Method				Clip Method			
			Training	Validation	Testing	Overall	Training	Validation	Testing	Overall
i.	3-input-based model	MSE	1.3421×10^{-3}	9.6157×10^{-4}	1.5935×10^{-3}	9.6158×10^{-4}	5.5103×10^{-3}	5.7986×10^{-3}	6.5508×10^{-4}	5.7986×10^{-3}
		R^2	0.9918	0.9950	0.9905	0.9921	0.9929	0.9926	0.9884	0.9915
ii.	5-input-based model	MSE	5.8034×10^{-4}	5.7790×10^{-4}	4.7800×10^{-4}	5.779×10^{-4}	5.1033×10^{-3}	3.7243×10^{-3}	4.2300×10^{-3}	3.7243×10^{-3}
		R^2	0.9971	0.9942	0.9932	0.9966	0.9929	0.9922	0.9945	0.9929
iii.	6-input-based model	MSE	8.2605×10^{-4}	8.7523×10^{-4}	7.2486×10^{-4}	8.7523×10^{-4}	3.0894×10^{-3}	6.9058×10^{-3}	2.4769×10^{-4}	3.8859×10^{-3}
		R^2	0.9949	0.9962	0.9955	0.9952	0.9953	0.9923	0.9955	0.9947

Generally, the computations of the neural network variables (i.e., inputs, weights, biases and output) in vector form are related, as represented in Equation 6 [65];

$$y_{ANN} = f_{out}\left[\sum_j Lw_{kj} \cdot f_{in}\left(\sum Iw_{ij}x_i + b_i\right) + b_k\right] \quad (6)$$

where y_{ANN} is the network predicted output (in normalized form), f_{out} denotes the output neuron activation function (i.e., *purelin*), Lw_{kj} represents the hidden layer neurons' weights from the *j*th neuron to the *k*th output layer neuron, f_{in} is the transfer function (*tansig*) at the hidden neuron, Iw_{ij} is the input layer weights from the *i*th neuron to the *j*th hidden layer neuron, and x_i represents an input variable. Then, b_i and b_k represent the hidden and output layers nodes' biases, respectively. Therefore, based on the established architectures for the neural network-based models for q_o prediction, their computation notations are presented in Equations 7 to 9; 3-input-based model:

$$(q_o)_{ANN} = \sum purelin\left\{\sum_{i=1}^{5}\sum_{j=1}^{3} t\,\text{an}\,sig\left[\left(P_{wh}j_1 + Sj_2 + GLRj_3\right)_i + b_i\right]\right\} \times Lw_{ij} + b_k \tag{7}$$

5-input-based model:

$$(q_o)_{ANN} = \sum purelin\left\{\sum_{i=1}^{6}\sum_{j=1}^{5} t\,\text{an}\,sig\left[\left(P_{wh}j_1 + Sj_2 + GLRj_3 + \left(T/T_{sc}\right)j_4 + BS\,\&\,Wj_5\right)_i + b_i\right]\right\} \times Lw_{ij} + b_k \tag{8}$$

6-input-based model:

$$(q_o)_{ANN} = \sum purelin\left\{\sum_{i=1}^{8}\sum_{j=1}^{6} t\,\text{an}\,sig\left[\left(P_{wh}j_1 + Sj_2 + GLRj_3 + \left(T/T_{sc}\right)j_4 + \gamma_o j_5 + \gamma_g j_6\right)_i + b_i\right]\right\} \times Lw_{ij} + b_k \tag{9}$$

where $(q_o)_{ANN}$ is the neural network predicted oil flow rate in normalized form. The variables j_1, j_2, j_3, j_4, j_5 and j_6 are the weights of the network inputs: P_{wh}, S, GLR, T/T_{sc}, $BS\&W$, γ_o and γ_g to the hidden layer neuron; Lw_{ij} represents the hidden layer weights that connect the output layer neuron; b_i and b_k are biases at the hidden and output neurons, respectively. Then, *purelin* and *tansig* are activation functions at the output and hidden layers' neurons. The weights and biases of the various neural network-based models for oil flow rate prediction are in Tables 6 to 11.

Table 6. *Weights and biases of the 3-input-based model using max.-min. scaling method.*

	Input layer weights			**Hidden biases and weights**		**Output bias**
i	$(P_{wh})\,j_1$	$(S)\,j_2$	$(GLR)\,j_3$	b_i	Lw_1	b_k
1	-0.5385402	-1.0111643	-0.3697213	1.974864	-1.1109503	-0.1585362
2	-1.2660117	5.7652163	2.0999111	-3.1918448	0.8373804	
3	0.29895761	1.3578018	-1.9698251	-2.8393038	5.1375123	
4	0.24131335	2.1912495	-0.5929832	-2.0673442	-2.6497395	
5	1.01553212	-1.3477269	1.15601166	3.3939060	3.6110957	

Table 7. *Weights and biases of the 3-input-based model using the clip scaling method.*

	Input layer weights			Hidden biases and weights		Output bias
i	$(P_{wh})\ j_1$	$(S)\ j_2$	$(GLR)\ j_3$	b_i	Lw_1	b_k
1	-1.9102399	0.1173669	-0.9406521	2.8339813	0.16789125	1.188847
2	2.1891470	-0.4798915	-3.5388877	-1.4183450	0.38368504	
3	0.7112502	2.47403781	-3.539615	-1.3528274	-0.28206409	
4	-1.0860498	-0.7007909	4.3089994	4.66603469	-2.55714526	
5	1.6228026	-2.7474310	-2.0315176	-2.3284541	-0.37376004	

Table 8. *Weights and biases of the 5-input-based model using max.-min. scaling method.*

	Input weights					Hidden biases	Hidden weights	Output bias
i	$(P_{wh})\ j_1$	$(S)\ j_2$	$(GLR)\ j_3$	$(T/T_{sc})\ j_4$	$(BS\&W)\ j_5$	b_i	Lw_1	b_k
1	3.4900924	-7.731092	-6.4360719	2.09776475	6.6313152	-11.863917	-2.3205470	0.3472364
2	3.4423928	-7.372197	-6.3975091	2.06356456	6.4071733	-11.511381	2.3664439	
3	0.0299627	1.7319449	-0.2676342	-0.56557378	-0.4638709	1.4411783	0.17676961	
4	0.8098289	1.0948423	-3.4110332	0.727664266	0.0829497	-4.0252434	1.6790642	
5	-7.188589	5.6356843	6.7863179	7.263317569	-0.5029194	-4.1082139	4.9673305	
6	-5.888010	4.8817139	0.50369342	6.2700012	-0.30080753	-8.6339629	-5.3101384	

Table 9. *Weights and biases of the 5-input-based model using the clip scaling method.*

	Input weights					Hidden biases	Hidden weights	Output bias
i	$(P_{wh})\ j_1$	$(S)\ j_2$	$(GLR)\ j_3$	$(T/T_{sc})\ j_4$	$(BS\&W)\ j_5$	b_i	Lw_1	b_k
1	0.9010532	0.6868277	-3.3368676	0.3989323	-0.0023792	-3.695982	1.7599079	0.662883
2	-0.994761	2.1941044	0.4255441	-3.6930451	1.69289456	3.0435556	0.1249966	
3	2.7616773	-2.832146	-2.1586329	-0.6128486	3.78528638	-2.1373435	0.0529069	
4	0.4204269	0.0523971	-1.1852713	-0.3920006	0.44395427	-0.655956	-0.2171184	
5	1.1663272	0.6718416	-2.0633890	-0.1329151	-0.1273617	0.2522338	0.133396	
6	-0.269904	-2.297810	1.6909864	0.3070311	-1.4469666	1.7310819	-0.0644734	

Table 10. *Weights and biases of the 6-input-based model using max.-min. scaling method.*

	Input weights						**Hidden biases**	**Hidden weights**	**Output bias**
i	$(P_{wh})\ j_1$	$(S)\ j_2$	$(GLR)\ j_3$	$(T/T_{sc})\ j_4$	$(\gamma_o)\ j_5$	$(\gamma_g)\ j_6$	b_i	Lw_1	b_k
1	0.047515	0.130103	0.44245	-2.030657	0.581165	-0.089446	1.970767	0.4357025	0.235916
2	-1.011681	0.891035	0.020582	-1.195120	-1.019611	-0.161630	1.139384	0.0776338	
3	0.316439	0.309080	-0.488147	1.140003	-0.367717	0.6344811	-0.450963	0.3284348	
4	-0.316973	-0.908201	0.045713	0.607017	-1.051208	-1.110216	-0.172092	-0.1304821	
5	0.632287	0.294746	-0.235050	-0.862207	-0.594977	-0.928184	0.637973	0.2560455	
6	0.594650	0.439590	-0.827425	-1.193106	0.6061402	0.1739179	1.484508	-0.260832	
7	-0.626795	0.869463	-0.980515	0.176416	-0.468085	-0.577010	-1.364878	-0.036701	
8	-0.560974	-0.483019	1.727690	-0.821655	-0.648451	-0.043607	2.329126	-1.3554218	

Table 11. *Weights and biases of the 6-input-based model using the clip scaling method.*

	Input weights						**Hidden biases**	**Hidden weights**	**Output bias**
i	$(P_{wh})\ j_1$	$(S)\ j_2$	$(GLR)\ j_3$	$(T/T_{sc})\ j_4$	$(\gamma_o)\ j_5$	$(\gamma_g)\ j_6$	b_i	Lw_1	b_k
1	-0.802896	1.032175	0.523643	1.267974	0.494186	-0.555345	2.146365	0.071464	-0.65368
2	-0.5326472	0.391553	0.265645	-1.635991	0.504839	-0.119175	-0.794149	-0.523327	
3	-0.000600	-0.864577	0.055065	0.576637	-0.537443	-0.721054	0.014171	-0.769143	
4	0.688203	2.37251	-1.50568	2.36764	0.877263	0.617937	0.603996	-0.068565	
5	0.523447	0.539761	-0.702578	2.091369	1.525157	0.449091	-1.461013	0.493293	
6	-0.832304	-0.934466	0.977342	-0.880203	-0.200528	0.809025	-1.422903	0.385712	
7	-1.877361	-0.722014	-0.02678	-0.280917	-0.139388	0.215438	-1.82908	-0.136098	
8	0.233416	0.240730	0.911708	-0.095287	-0.241667	-1.41470	2.185845	0.587712	

Aside from the network architectures, as visible in Figures 3 to 5, the weights and biases (Tables 5 to 10), and other details of the networks, it is imperative to establish the average contribution of the input variables on the network output [60, 66]. This average contribution of input parameters on the network output is the contribution factor (CF) or relative importance (RI). Thus, the Garson method expanded in Equation 10 to determine the RI of the input variables on the neural network's output [60].

$$RI = \frac{\sum_{j}^{n_i}\left(\frac{|Lw_{ij}|}{\sum_{k}^{I_m}|Lw_{ij}|} Iw_i\right)}{\sum_{i}^{I_m}\sum_{j}^{n_i}\left(\frac{|Lw_{ij}|}{\sum_{k}^{I_m}|Lw_{ij}|} Iw_i\right)} \times 100\% \quad (10)$$

where Iw_i is the input layer weights, Lw_{ij} denotes the hidden layer weights to the output neuron, n_i and I_m represent the numbers of inputs and hidden layer's neurons. The outcomes of the RI assessment on the networks' input variables are in Table 12.

The results from the RI assessment in Table 12 revealed that the bean (choke) size and GLR are the most significant parameters in the developed neural networks for oil flow rate prediction. The observation aligns with the position of Joshua et al. [26]. Also, it revealed that the dataset scaling (normalization) approach influenced the input variables' RI on the networks' output. This observation is visible in the RI ranking of the network input variables in Table 12. The 3-input-based network had an RI ranking of S>GLR>P_{wh} for the maximum-minimum scaling method and an RI ranking of GLR>S>P_{wh} for the clip scaling approach. The 5-input-based network had an RI ranking of S>GLR>T/T_{sc}>P_{wh}>BS&W for the maximum-minimum normalization approach and GLR>S>P_{wh}>BS&W>T/T_{sc} for the clip method. Likewise, the 6-input-based network resulted in T/T_{sc}>γ_o>GLR>S>P_{wh}>γ_g and T/T_{sc}>S>P_{wh}>γ_g>GLR>γ_o for maximum-minimum and clip methods, respectively. Thus, the overall RI ranking of the input variables on the developed networks' output is S>GLR>P_{wh}>T/Tsc> γ_o>BS&W>γ_g.

Table 12. *Relative importance ranking of the neural-based models' input variables.*

	Model	Scaling method	Input Variables Relative Importance (%)						
			P_{wh}	S	GLR	T/T_{sc}	BS&W	γ_o	γ_g
i.	3-input-based	Max.-min.	17.40	52.80	28.80	NA	NA	NA	NA
		RI ranking	3rd	1st	2nd	NA	NA	NA	NA
		Clip	26.01	26.64	47.35	NA	NA	NA	NA
		RI ranking	3rd	2nd	1st	NA	NA	NA	NA
ii.	5-input-based	Max.-min.	16.68	30.07	23.56	18.00	11.69	NA	NA
		RI ranking	4th	1st	2nd	3rd	5th	NA	NA
		Clip	16.68	19.51	35.06	12.93	15.82	NA	NA
		RI ranking	3rd	2nd	1st	5th	4th	NA	NA
iii.	6-input-based	Max.-min.	13.24	13.90	15.62	27.29	NA	17.36	12.59
		RI ranking	5th	4th	3rd	1st	NA	2nd	6th
		Clip	16.59	19.02	12.72	23.76	NA	12.20	15.71
		RI ranking	3rd	2nd	5th	1st	NA	6th	4th

*NA = not applicable

3.2. Simplified Neural Network-Based Models for Oil Flow Rate Prediction

According to Okon et al. [60], numerous researchers have presented neural networks in "black box" form. The developed neural models are not in a simplified mathematical form. This drawback limits the ability of ardent readers to understand the application of any developed neural network model [46]. Okon et al. [62] presented detailed workings of the neural network to achieve its prediction (output) from the input variables. Considering the 3-input-based network, the basic neural network computations steps are as follows [67]:

1) input variables (P_{wh}, S and GLR) from the input neurons multiply with input weights (j_1, j_2 and j_3), respectively, and are linked to hidden layer neurons;
2) at the first hidden layer neuron (i.e., i = 1), the input (i.e., $P_{wh}j_1 + Sj_2 + GLRj_3$) from the input layer combined with the neuron's bias (b_i) and the sum (i.e., $\sum_{i=1}\left(P_{wh}j_1 + Sj_2 + GLRj_3\right) + b_i$) is transformed by the sigmoid function (Equation 11), to the output neuron;

$$\sigma\left(z_i\right) = \frac{2}{1+e^{-2(\beta_i)}} - 1 \tag{11}$$

where β_i is $\sum_{i=1}\left(P_{wh}j_1 + Sj_2 + GLRj_3\right) + b_i$

3) the transformed output from the hidden neuron (i.e., $\sigma(z_i)$) multiplied by the hidden neuron weight (Lw_i) and linked to the output neuron;
4) at the output neuron, the hidden layer output combined with its bias (b_k), thus, $\left(\sigma(z_i)\times Lw_i\right)+b_k$;
5) steps (i) to (iv) are repeated for values of i = 2,...5 for the neurons and at the output neuron, the sum $\sum_{j=1}^{5}\sum_{i=1}^{3}\left[\left(\sigma(z_i)\times Lw_i\right)+b_k\right]$ is transformed using the *purelin* function as the network's output. Thus, the predicted values are $purelin\sum_{j=1}^{5}\sum_{i=1}^{3}\left[\left(\sigma(z_i)\times Lw_i\right)+b_k\right]$.

The values for the variables j_1, j_2, j_3, b_i, Lw_i and b_k are in Tables 5 and 6, and they could be applied to other networks (i.e., 5-input-based and 6-input-based) with appropriate adjustments to the network's variables. The output from the neural network is presented in the normalized form and would require de-normalization to transform the network predictions to a required format (values). Thus, the simplified neural network-based models for oil flow rate prediction are in Equations 12 and 13, based on maximum-minimum and clip scaling approaches;

$$q_o = 183 + 14234\left(q_{o_{MS}}\right)_{ANN} \tag{12}$$

$$q_o = 7300 + 7117\left(q_{o_{CS}}\right)_{ANN} \tag{13}$$

where q_o is the de-normalized oil flow rate, $\left(q_{o_{MS}}\right)_{ANN}$ and $\left(q_{o_{CS}}\right)_{ANN}$ are the predicted oil flow rates (in normalized form) based on the maximum-minimum and the clip scaling methods, respectively, from the neural network. Thus, $\left(q_{o_{MS}}\right)_{ANN}$ and $\left(q_{o_{CS}}\right)_{ANN}$ are expressed in Equations 14 and 15;

$$\left(q_{o_{MS}}\right)_{ANN} = \left[-1.11095\sigma(z_1) + 0.83738\sigma(z_2) + 5.13751\sigma(z_3) - 2.64974\sigma(z_4) + 3.6111\sigma(z_5)\right] - 0.15854 \tag{14}$$

$$\left(q_{o_{CS}}\right)_{ANN} = \left[0.16789\sigma(z_1) + 0.38369\sigma(z_2) - 0.28206\sigma(z_3) - 2.55715\sigma(z_4) - 0.37376\sigma(z_5)\right] - 1.18885 \tag{15}$$

Then, $\sigma(z_1)$ to $\sigma(z_5)$ in Equations 14 and 15 are expressed as $\sigma(z_1) = \frac{2}{1+e^{-2(\beta_1)}} - 1$, $\sigma(z_2) = \frac{2}{1+e^{-2(\beta_2)}} - 1$, $\sigma(z_3) = \frac{2}{1+e^{-2(\beta_3)}} - 1$, $\sigma(z_4) = \frac{2}{1+e^{-2(\beta_4)}} - 1$ and $\sigma(z_5) = \frac{2}{1+e^{-2(\beta_5)}} - 1$, where β_1 to β_5 are the computations at the hidden layer neurons. For the 3-input-based network with the maximum-minimum scaling method, β_1 to β_5 are expanded as Equations 16 to 20;

$$\beta_1 = \left[-0.53854\left(P_{wh}\right)_n - 1.01116\left(S\right)_n - 0.36972\left(GLR\right)_n\right] + 1.97486 \tag{16}$$

$$\beta_2 = \left[-1.26601\left(P_{wh}\right)_n + 5.76522\left(S\right)_n + 2.09991\left(GLR\right)_n\right] - 3.19185 \tag{17}$$

$$\beta_3 = \left[0.29896\left(P_{wh}\right)_n + 1.35780\left(S\right)_n - 1.96983\left(GLR\right)_n\right] - 2.83930 \tag{18}$$

$$\beta_4 = \left[0.24131\left(P_{wh}\right)_n + 2.19125\left(S\right)_n - 0.59298\left(GLR\right)_n\right] - 2.06734 \tag{19}$$

$$\beta_5 = \left[1.01553\left(P_{wh}\right)_n - 1.34773\left(S\right)_n + 1.15601\left(GLR\right)_n\right] + 3.39391 \tag{20}$$

Also, the variables β_1 to β_5 for the 3-input-based network with the clip scaling method are expressed as Equations 21 to 25;

$$\beta_1 = \left[-1.91024\left(P_{wh}\right)_n + 0.11737\left(S\right)_n - 0.94065\left(GLR\right)_n\right] + 2.83398 \tag{21}$$

$$\beta_2 = \left[2.18915\left(P_{wh}\right)_n - 0.47989\left(S\right)_n - 3.53889\left(GLR\right)_n\right] - 1.41835 \quad (22)$$

$$\beta_3 = \left[0.71125\left(P_{wh}\right)_n + 2.47404\left(S\right)_n - 3.53962\left(GLR\right)_n\right] - 1.35283 \quad (23)$$

$$\beta_4 = \left[-1.08605\left(P_{wh}\right)_n - 0.70079\left(S\right)_n + 4.30899\left(GLR\right)_n\right] + 4.66605 \quad (24)$$

$$\beta_5 = \left[1.62280\left(P_{wh}\right)_n - 2.74743\left(S\right)_n - 2.03152\left(GLR\right)_n\right] - 2.32845 \quad (25)$$

where $\left(P_{wh}\right)_n$, $\left(S\right)_n$, and $\left(GLR\right)_n$ are the normalized input variables (i.e., P_{wh}, S, and GLR), presented as $\left(P_{wh}\right)_n = \frac{P_{wh} - 95}{3205}$, $\left(S\right)_n = \frac{S - 14}{60}$, and $\left(GLR\right)_n = \frac{GLR - 29}{28568}$, for the maximum-minimum scaling method and $\left(P_{wh}\right)_n = 2\left(\frac{P_{wh} - 95}{3205}\right) - 1$, $\left(S\right)_n = 2\left(\frac{S - 14}{60}\right) - 1$, and $\left(GLR\right)_n = 2\left(\frac{GLR - 29}{28568}\right) - 1$, for the clip scaling method.

Similarly, the 5-input-based and 6-input-based models' $\left(q_{o_{MS}}\right)_{ANN}$ and $\left(q_{o_{CS}}\right)_{ANN}$ are adjusted to reflect the additional input parameters: T/T_{sc}, $BS\&W$, γ_o and γ_g. Using the appropriate weights and biases presented in Tables 8 and 9 for 5-input-based models and Tables 10 and 11 for 6-input-based models, $\sigma\left(z_i\right)$ and β_i would be established. The normalized additional input variables are expressed as $\left(T/T_{sc}\right)_n = \frac{T/T_{sc} - 0.8}{2.30}$, $\left(BS\&W\right)_n = \frac{BS\&W - 0.0005}{0.9425}$, $\left(\gamma_o\right)_n = \frac{\gamma_o - 0.7339}{0.2094}$ and $\left(\gamma_g\right)_n = \frac{\gamma_g - 0.5227}{0.4172}$ for the maximum-minimum normalization method and $\left(T/T_{sc}\right)_n = 2\left(\frac{T/T_{sc} - 0.8}{2.30}\right) - 1$, $\left(BS\&W\right)_n = 2\left(\frac{BS\&W - 0.0005}{0.9425}\right) - 1$, $\left(\gamma_o\right)_n = 2\left(\frac{\gamma_o - 0.7339}{0.2094}\right) - 1$ and $\left(\gamma_g\right)_n = 2\left(\frac{\gamma_g - 0.5227}{0.4172}\right) - 1$ for the clip scaling method.

3.3. Comparison of the Simplified Models with Some Empirical Correlations for Oil Flow Rate Estimation

The predictions of the simplified neural network-based models were compared with some empirical correlations for oil flow rate (q_o) estimations. The performance of (i.e., the closeness between) the models predicted q_o with the actual field data was related using some statistical indices: coefficient of determination (R^2), root mean square error (RMSE), average relative error (ARE) and average absolute relative error (AARE), and regression plot. The statistical indices are estimated using Equations 26 to 31:

$$R^2 = 1 - \frac{\sum_{i=1}^{n}\left(q_{o_{field}} - q_{o_{pred.}}\right)^2}{\sum_{i=1}^{n}\left(q_{o_{field}} - \overline{q_{o_{pred.}}}\right)^2} \quad (26)$$

$$RMSE = \sqrt{\frac{1}{n}\sum_{i=1}^{n}\left(q_{o_{field}} - q_{o_{pred.}}\right)^2} \quad (27)$$

$$ARE = \frac{1}{n}\sum_{i=1}^{n}\left(\frac{q_{o_{pred.}} - q_{o_{field}}}{q_{o_{field}}}\right) \quad (28)$$

$$AARE = \frac{1}{n}\sum_{i=1}^{n}\left|\frac{q_{o_{pred.}} - q_{o_{field}}}{q_{o_{field}}}\right| \quad (29)$$

where $q_{o_{field}}$ and $\overline{q_{o_{field}}}$ denote the field oil flow rate and average field flow rate, respectively, $q_{o_{pred.}}$ and $\overline{q_{o_{pred.}}}$ represent the predicted oil flow rate and average predicted oil flow rate, respectively, from the neural-based models, and n denotes the number of datasets or data points.

The 3-input-based models' (i.e., ANN-MS and ANN-CS) predictions and other empirical correlations: Gilbert [14], Baxendell [15], Ros [16], Achong [17], Owolabi et al. [20], Beiranvand et al. [4], Okon et al. [23] and Joshua et al. [26], estimations were collated. The results are in Table 13 and Figures 10 and 11. In Table 13, the neural network-based models have the lowest statistical indices (i.e., RMSE, ARE and AARE) compared to the empirical correlations. The developed neural network model based on the maximum-minimum normalization approach (ANN-MS) resulted in an R^2 value of 0.9687, while the model based on the clip scaling method resulted in an R^2 value of 0.9663. The R^2 values for the ANN-MS and ANN-CS models were higher than the performance of the empirical correlations, even for the corre-

lations (Owolabi et al. [20]; Okon et al. [23]; Joshua et al. [26]) based on the Niger Delta region. Statistically, these high R^2 values for the neural network-based models implied that their predictions would fit closer to the actual field data than the estimation of the empirical correlations [60]. Besides the statistical indicators in Table 13, the Taylor diagram of the 3-input-based models and empirical correlations is presented in Figure 10. This figure shows the statistical errors and agreement of the developed models and the empirical correlations with the field data [68, 69]. Thus, the predictions of the field data by the 3-input-based models (i.e., ANN-MS and ANN-CS) are more noticeable than the empirical correlations in Figure 10. Again, Figure 11 depicts the predictions of the neural models and empirical correlations with the field q_o. The figure indicates that the neural and empirical correlations estimated data points aligned along the diagonal trend in Figure 11. According to Al-Bulushi et al. [64], the diagonal alignment of the neural-based model predictions and the estimation of the empirical correlations with the field q_o shows a good agreement between the predicted q_o and the actual field q_o datasets.

Table 13. *Statistical performance of the developed Gilbert-based models with some empirical correlations for oil flow rate estimation.*

	Models	Statistical Performance			
		R^2	RMSE	ARE	AARE
i.	Gilbert (1954)	0.8717	1056.088	-0.1268	0.3177
ii.	Baxendell (1958)	0.9329	759.155	0.2513	0.3734
iii.	Ros (1960)	0.9402	716.155	0.1688	0.3354
iv.	Achong (1961)	0.8939	962.841	0.3927	0.4872
v.	Owolabi et al. (1991)	0.9073	970.250	0.3358	0.5766
vi.	Beiranvand et al. (2012)	0.9386	726.693	-0.0264	0.3002
vii.	Okon et al. (2014)	0.9627	877.850	0.4330	0.5187
viii.	Joshua et al. (2020)	0.9477	669.982	0.0547	0.2998
ix.	ANN-MS	0.9687	517.719	0.1012	0.2468
x.	ANN-CS	0.9663	537.677	0.0673	0.2582

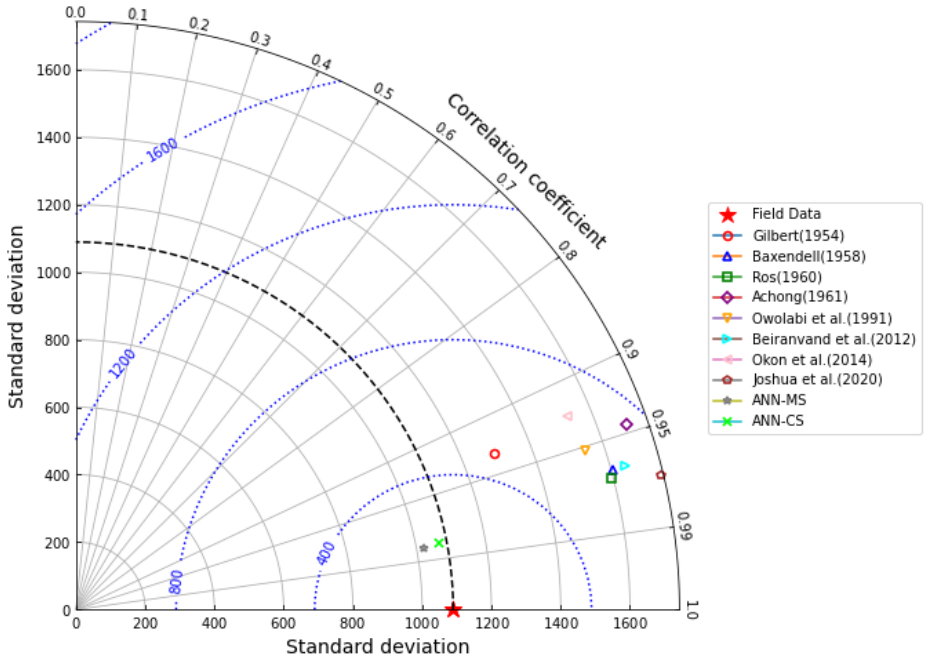

Figure 10. *Taylor diagram of the 3-input-based models with some empirical correlations.*

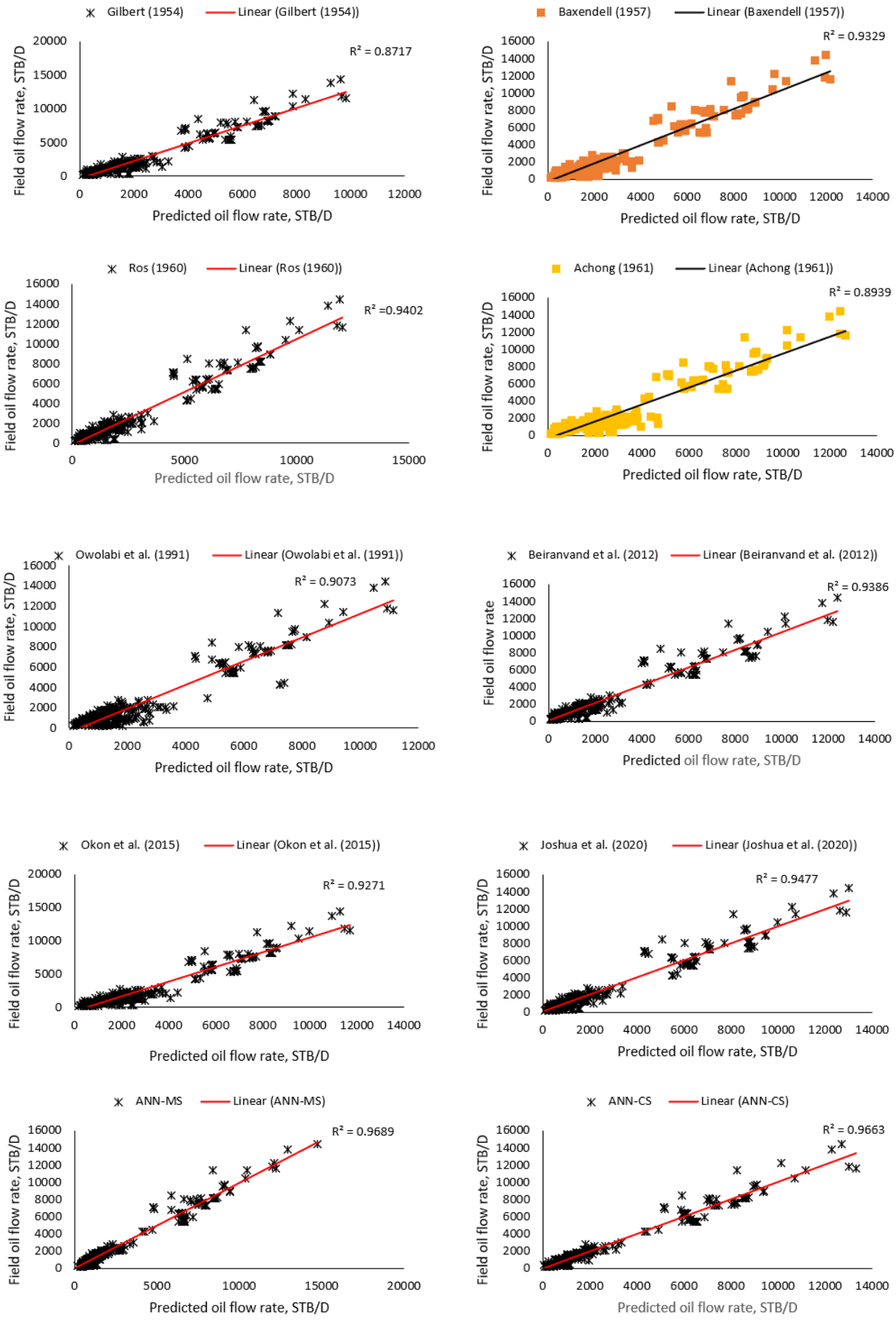

Figure 11. *Comparison of the 3-input-based neural models and empirical correlations predictions; the diagonal line represents 1:1 trend line.*

On the other hand, Table 14 presents the statistical performance (i.e., R^2, RMSE, ARE and AARE) of the 5-input neural-based models and some empirical correlations. The results showed that the simplified neural-based models' (i.e., ANN-MS and ANN-CS) statistical yardsticks were better than the empirical correlations by Beiranvand et al. [4], Khorzoughi et al. [22], Okon et al. [23] and Ghorbani et al. [24]. This assertion is revealed in the R^2 values obtained for the 5-input neural-based models. In Table 14, the ANN-MS model had an R^2 value of 0.9867, while the ANN-CS model resulted in an R^2 value of 0.9720. These R^2 values implied that the 5-input neural-based models would predict the field q_o with 98.67% and 97.20% for ANN-MS and ANN-CS models, respectively. Also, the RMSE, ARE, and AARE values obtained for the neural-based models were lesser than the empirical correlations' estimations. Furthermore, the performance of the neural network-based models and the empirical correlations are in Figure 12. From the figure, the neural-based models and some correlations: Beiranvand et al. [4], Okon et al. [23], and Ghorbani et al. [24] predictions cluster along the diagonal trend. The figure reveals that the estimated correlation values between Khorzoughi et al. [22] did not agree with the actual field q_o. The observation is visible in the data points (trend) for Khorzoughi et al. [22] correlation in Figure 12 and the R^2 value obtained for the correlation in Table 14.

Table 14. *Statistical performance of the developed 5-input-based models with some empirical correlations for oil flow rate estimation.*

	Models	Statistical Performance			
		R^2	RMSE	ARE	AARE
i.	Beiranvand et al. [4]	0.9468	718.010	0.1737	0.3300
ii.	Khorzoughi et al. [22]	0.6560	2229.569	0.4601	0.7499
iii.	Okon et al. [23]	0.9023	1253.268	0.5515	0.6486
iv.	Ghorbani et al [24]	0.9255	926.690	-0.1040	0.3742
v.	ANN-MS	0.9867	383.276	0.1139	0.2367
vi.	ANN-CS	0.9720	491.487	0.1144	0.2642

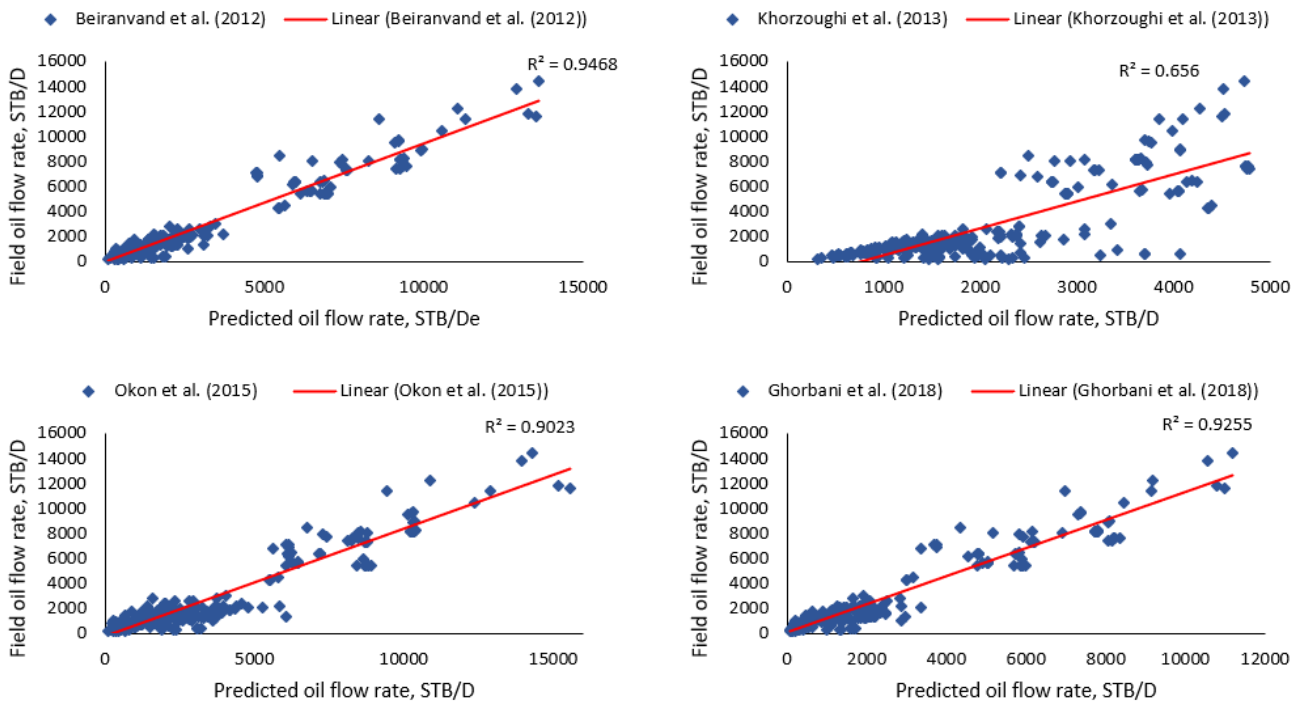

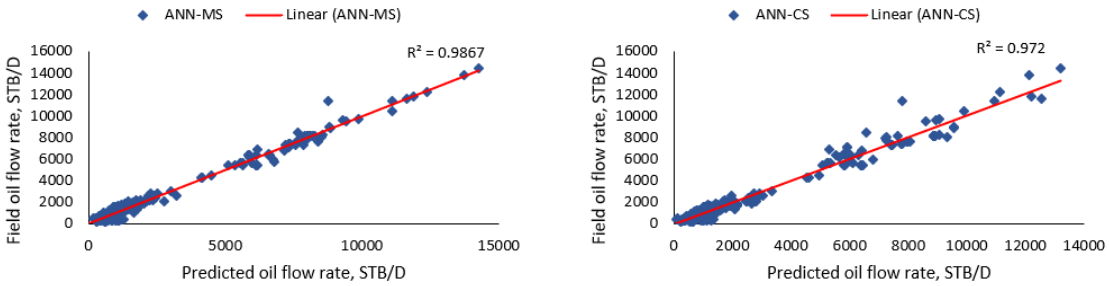

Figure 12. *Comparison of the 5-input-based neural models and empirical correlations predictions; the diagonal line represents 1:1 trend line.*

Table 15 presents the statistical performance of the 6-input-based neural network models and some empirical correlations: Choubineh et al. [12] and Joshua et al. [26]. The results (i.e., R^2 values) indicated that the prediction of the neural network-based models was closer to the actual field q_o than the empirical correlation estimations. Again, the error indicators (i.e., RMSE, ARE and AARE values) for the neural-based models were lesser than those obtained for the empirical correlations. Also, the neural models' predictions aligned diagonally more than the empirical correlations' estimations in Figure 13. The observation implied that the neural-based models' predictions were in sync with the actual field datasets, with 98.08% and 97.91% certainty for the ANN-MS and ANN-CS models, respectively.

Table 15. *Statistical performance of the 6-input-based models with some empirical correlations for oil flow rate estimation.*

	Models	Statistical Performance			
		R^2	RMSE	ARE	AARE
i.	Choubineh et al. [12]	0.9443	721.958	0.0892	0.3316
ii.	Joshua et al. [26]	0.9749	1089.123	0.3833	0.4196
iii.	ANN-MS	0.9808	407.186	0.0643	0.2192
iv.	ANN-CS	0.9791	424.931	0.0425	0.2594

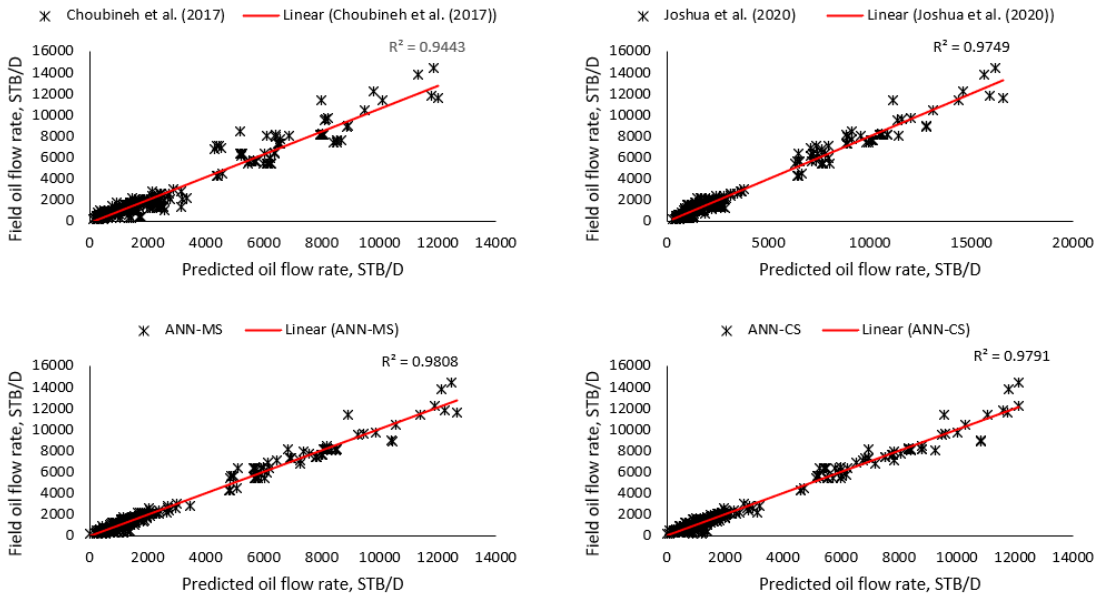

Figure 13. *Comparison of the 6-input-based neural models and empirical correlations predictions; the diagonal line represents 1:1 trend line.*

3.4. Generalization Performance of the Simplified Neural Network-Based Models for Oil Flow Rate Predictions

According to Alexander et al. [70], applying datasets not involved in developing the model to assess its generalization robustness is the gold standard. In this regard, 63 and 113 datasets from the Niger Delta and Iran fields, respectively, in Okon et al. [23] and Choubineh et al. [12], were used for the assessment. Tables 16 and 17 show the statistical description of the datasets. The generalization performances of the simplified 3-input-based and 6-input-based neural models were tested using these datasets. The models' performance is visible in statistical indices (i.e., R^2, RMSE, ARE and AARE) in Tables 18 and 19 and regression plots in Figures 14 to 19.

Table 16. *Statistical description of Okon et al. [23] datasets for the models' generalization performance.*

Parameters	Data	Max.	Min.	Range	Mean	Std. Dev.	Kurt.	Coef. of Var. (%)
Wellhead Pressure, P_{wh}	63	2320.0	101.5	2218.6	592.93	445.31	2.957	75.10
Bean (Choke) Size, S	63	72.0	16.0	56.0	35.46	13.96	0.268	39.38
Gas-Liquid Ratio, GLR	63	4134.41	93.26	4041.15	889.64	925.15	4.802	103.99

Table 17. *Statistical description of Choubineh et al. [12] datasets for the models' generalization performance.*

Parameters	Data	Max.	Min.	Range	Mean	Std. Dev.	Kurt.	Coef. of Var. (%)
Wellhead Pressure, P_{wh}	113	2940.0	50.0	2890.0	1280.1	348.69	1.275	77.13
Bean (Choke) Size, S	113	80.0	24.0	56.0	54.51	16.88	0.122	43.89
Gas-Liquid Ratio, GLR	113	3660.0	107.0	3553.0	858.58	440.25	8.518	206.33
Oil Gravity, γ_o	113	0.92	0.808	0.112	0.8583	0.0171	-0.047	5.30
Temperature, T	113	135.0	90.0	45.0	124.12	12.61	0.384	29.81
Gas Gravity, γ_g	113	1.236	0.6886	0.5474	0.7313	0.0597	-0.805	3.14

Table 18 and Figures 14 to 17 present the 3-input-based neural models (i.e., ANN-MS and ANN-CS) generalization performance with the Okon et al. [23] and Choubineh et al. [12] datasets. For the Okon et al. [23] datasets, the statistical indicator showed that the neural-based models predicted q_o resulted in R^2 values of 0.9488 for ANN-MS, while the ANN-CS model had 0.9644. From a statistical standpoint, the R^2 values implied that the simplified neural-based models predicted q_o are 94.88% (for ANN-MS) and 96.44% (for ANN-CS) related to the Okon et al. [23] datasets. The results further depict RMSE, ARE, and AARE values of 251.926, 0.1158, and 0.1862 for the ANN-MS model and 205.871, 0.1158, and 0.1862 for the ANN-CS model. Again, the 3-input-based neural model predictions from the Choubineh et al. [12] datasets resulted in R^2 values of 0.8848 for the ANN-MS model and 0.9264 for the ANN-CS model. The errors (i.e., RMSE, ARE, and AARE) values obtained for the models were 2754.48, 0.0746 and 0.2573 for ANN-MS and 2089.93, 0.1656 and 0.2267 for ANN-CS. From the R^2 values obtained, the simplified 3-input-based neural models would predict Choubineh et al. [12] q_o datasets with 88.48% and 92.64% certainty for ANN-MS and ANN-CS models, respectively. Aside from the R^2 values that depict the predicted q_o 's closeness with the test datasets, the generality robustness of these simplified neural-based models is visible on the cross-plots in Figures 14 to 17. As observed in these figures, the diagonal trend of the data points indicates a good agreement between the predicted q_o and the test datasets [64].

Table 18. *Statistical indices of the simplified 3-input-based models' generalization robustness to predict the oil flow rate.*

	Datasets Source	Neural Model	Statistical Performance			
			R^2	RMSE	ARE	AARE
i.	Okon et al. [23]	ANN-MS	0.9488	251.926	0.1158	0.1862
		ANN-CS	0.9644	205.781	0.0248	0.1275
ii.	Choubineh et al. [12]	ANN-MS	0.8848	2754.48	0.0746	0.2573
		ANN-CS	0.9264	2089.93	0.1656	0.2267

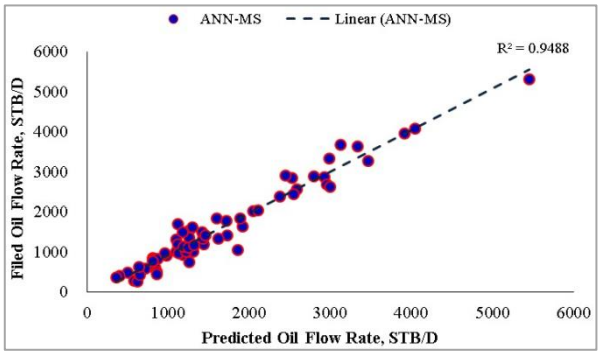

Figure 14. *Comparison of 3-input-based model (ANN-MS) predictions with oil flow rate datasets from Okon et al. [23].*

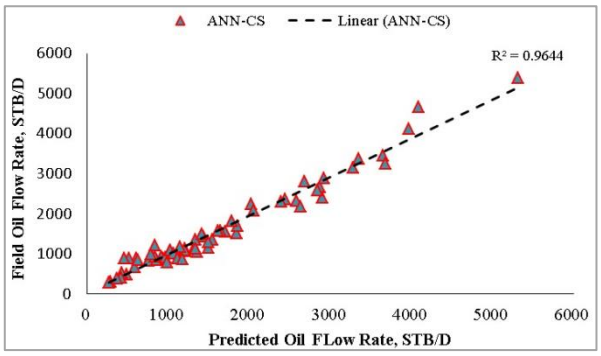

Figure 15. *Comparison of 3-input-based model (ANN-CS) predictions with oil flow rate datasets from Okon et al. [23].*

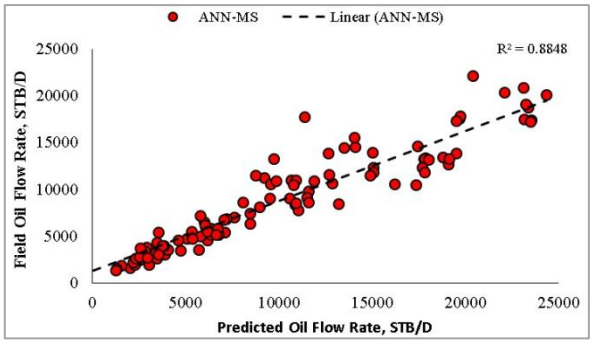

Figure 16. *Comparison of 3-input-based model (ANN-MS) predictions with oil flow rate datasets from Choubineh et al. [12].*

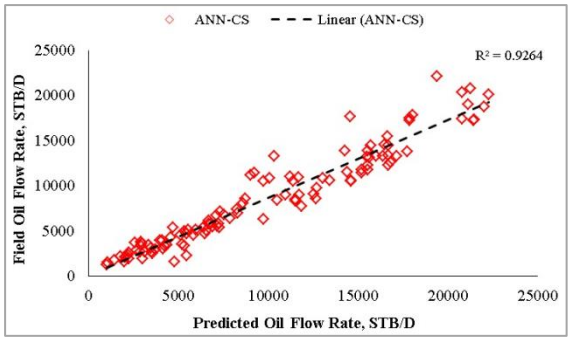

Figure 17. *Comparison of 3-input-based model (ANN-CS) predictions with oil flow rate datasets from Choubineh et al. [12].*

On the other hand, the 6-input neural-based models' generality performances are presented in Table 19 and Figures 18 and 19. The statistical indices obtained for these models were 0.8908, 2655.50, 0.1484, and 0.2219 for R^2, RMSE, ARE, and AARE for ANN-MS, while ANN-CS had 0.9264, 2089.93, 0.1656 and 0.2267. The R^2 values obtained indicated that the 6-input-based neural models would predict the Choubineh et al. [12] q_o data with 89.08% certainty for ANN-MS and 92.64% for ANN-CS. Also, the closeness of the model's predictions with the test datasets is visible on the diagonal alignment of the predicted q_o and test datasets in the cross-plots (Figures 18 and 19). Thus, the generalization performance of the simplified neural-based models is about 90.0% certainty with the test datasets.

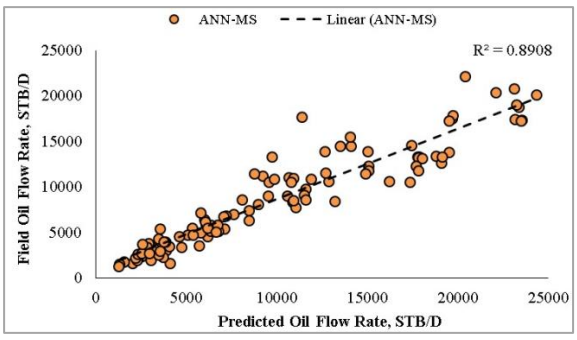

Figure 18. *Comparison of 6-input-based model (ANN-MS) predictions with oil flow rate datasets from Choubineh et al. [12].*

Table 19. *Statistical indices of the simplified 6-input-based models' generalization robustness to predict the oil flow rate.*

	Datasets Source	Neural Model	Statistical Performance			
			R^2	RMSE	ARE	AARE
i.	Choubineh et al. [12]	ANN-MS	0.8908	2655.50	0.1484	0.2219
		ANN-CS	0.9264	2089.93	0.1656	0.2267

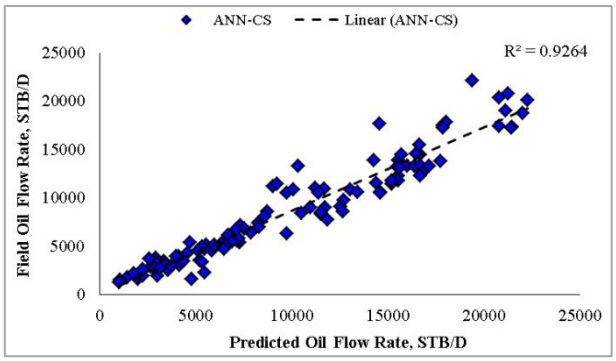

Figure 19. *Comparison of 6-input-based model (ANN-CS) predictions with oil flow rate datasets from Choubineh et al. [12].*

The generalization performance of Okon et al. [23] and Choubineh et al. [12] datasets was extended to some existing empirical correlations and compared with the simplified neural-based models. The results of the assessment are in Tables 20 and 21. In Table 20, the statistical results (R^2, RMSE, ARE and AARE) for the Okon et al. [23] datasets showed that the simplified 3-input-based neural models predicted q_o values were closer to the actual test datasets than the estimated q_o from the empirical correlations. The neural-based models' predictions for the Choubineh et al. [12] test data agreed with the estimated q_o from the empirical correlations as the R-values obtained for these models were close. On the other hand, the simplified 6-input-based neural models' generalization performance was comparable with the correlations of Choubineh et al. [12] and Joshua et al. [26]. This observation is visible in the statistical indices in Table 21 obtained for the neural-based models and the empirical correlations.

Table 20. *Generalization performances of the simplified 3-input-based models and some correlations with test datasets.*

	Models	Statistical Performance							
		Okon et al. (2015). Datasets				Choubineh et al. (2017) Datasets			
		R^2	RMSE	ARE	AARE	R^2	RMSE	ARE	AARE
i.	Gilbert [14]	0.5099	944.51	-0.4403	0.3349	0.8117	2451.04	0.1957	-0.1924
ii.	Baxendell [15]	0.5062	1120.79	0.0504	0.3254	0.9596	1130.74	-0.0110	0.0904
iii.	Ros [16]	0.5070	1111.48	-0.0093	0.3182	0.9548	1138.66	0.0261	0.0941
iv.	Achong [17]	0.4805	1218.12	0.1445	0.3665	0.9555	1128.76	0.0161	0.0989
v.	Pilehvari [19]	0.4977	2971.07	0.8235	0.8828	0.9394	10379.76	0.9623	0.9623
vi.	Beiranvand et al. [4]	0.4574	1210.70	-0.1398	0.3833	0.9495	1205.77	0.0868	0.1339
vii.	Okon et al. [23]	0.5319	1053.51	0.1658	0.3660	0.9345	1371.86	0.0157	0.1154
viii.	Owolabi et al. [20]	0.5210	1059.91	0.0323	0.3461	0.9302	141620	-0.0023	0.1184
ix.	Joshua et al. [26]	0.4821	1246.46	-0.0756	0.3469	0.9334	1383.10	-0.0010	0.1234
x.	ANN-MS	0.9488	251.926	0.1158	0.1862	0.8848	2754.48	0.0746	0.2573
xi.	ANN-CS	0.9644	205.781	0.0248	0.1275	0.9264	2089.93	0.1656	0.2267

Table 21. *Generalization performances of the simplified 6-input-based models and some correlations with test datasets.*

	Models	Statistical Performance			
		R^2	RMSE	ARE	AARE
i.	Choubineh et al. [12]	0.9695	1077.45	-0.0089	0.0941
ii.	Joshua et al. [26]	0.8949	1786.34	0.2262	0.2450
iii.	ANN-MS	0.8908	2655.50	0.1484	0.2219
iv.	ANN-CS	0.9264	2089.93	0.1656	0.2267

3.5. Statistical Significance and Acceptability of the Developed Models Predictions

In addition to the earlier-mentioned statistical indicators, which are parametric statistical tests to evaluate the performance of the developed neural network-based models, the Kruskal-Wallis test (i.e., H-test or H_{stat}), a non-parametric method alternative to the one-way analysis of variance (ANOVA), was evaluated using Equation 30 to test whether the models' predicted and field test oil flow rate datasets have the same mean values. Therefore, the null hypothesis ($*H_0$) is whether a significant difference exists between predicted models and the field oil flow rate mean values.

$$H_{stat} = \left[\frac{12}{N(N+1)}\sum_{i=1}^{k}\left(\frac{R_i^2}{n_i}\right)\right] - 3(N+1) \qquad (30)$$

where H_{stat} is the H-test value, which is equivalent to the critical value of Chi-square (χ^2), N represents the total number of data points in the test, k denotes the number of data groups in the test, R_i is the rank sum of the individual group in the test and n_i is the number of data points in each group.

Table 22 presents the Kruskal-Wallis test results at a 95% significance level for the field test, Okon et al. [23] and Choubineh et al. [12] datasets compared with the developed models predicted values. Based on the H_{stat} values obtained, which are equivalent to the critical values of Chi-square (χ^2). Based on the critical values table, at 2 degrees of freedom, the corresponding p-values visible in Table 22 for the H_{stat} values are less than the p-value of 0.05. Therefore, the null hypothesis ($*H_0$) that no significant difference exists between the models predicted and field test oil flow rate mean values are accepted. Hence, the developed models (ANN-MS and ANN-CS) predictions of oil flow rate are statistically significant and acceptable.

Table 22. *Kruskal-Wallis test of the models predicted and field test oil flow rate 95% significance level.*

	Datasets source	H_{stat} values	p-values	Null hypothesis ($*H_0$)
i.	Field test	6.6721	0.0377	Accept
ii.	Okon et al. [23]	6.5562	0.0398	Accept
iii.	Choubineh et al. [12]	7.6463	0.0478	Accept

In summary, the study has put forward simplified 3-input, 5-input, and 6-input neural-based models based on Gilbert [14], Khorzoughi et al. [22], and Choubineh et al. [12] correlations for Niger Delta oilfield flow rate prediction. Extending the generalization performances of the neural-based models to Iran oilfield datasets resulted in an excellent performance that compares with the Choubineh et al. [12] correlation. However, it is expedient to state that the unavailability or accessibility of datasets from oilfields across the globe for training and development of neural-based models would limit their application in other oil-producing regions. Again, it was alluded that most available neural network models for oil flow rate prediction in Table 1 have complex structures (architectures), making their implementation time-consuming. Moreover, these models' reproducibilities are doubtful, as the authors did not report the details of their

models (networks) to reproduce them for applications. Therefore, the gains of this study showed that:

1) the neural networks are reproducible as their basic details and network arrangement are presented in this study;
2) the neural network models are not reported as "black boxes" but rather as "white boxes," meaning the mathematical expressions of the networks' computations are presented,
3) clip normalized neural-based model generalizes unseen datasets more than the maximum-minimum neural-based model;
4) the parametric (relative) importance of the neural-based models' input variables on the output variable - oil flow rate is normalization approach sensitive;
5) the bean (choke) size (S), gas-liquid ratio (GLR), wellhead pressure (P_{wh}), well-flowing temperature (T) and oil gravity (γ_o) are more substantial in predicting oil flow rate (q_o) than basic sediments and water (BS&W) and gas gravity (γ_g); and
6) This work should consider the simplified representation of the neural-based models and the models' details for application.

4. Conclusion

The available intelligence-based models for oil flow rate in the Niger Delta region are not reproducible, as the models' basic details for their reproducibility are not published or in the public domain. In other words, the available models are viewed or presented as a black box. Therefore, this study showcases the simplified neural-based models based on 3-input, 5-input and 6-input parameters for predicting oil flow rate using 283 datasets from 21 wells in the Niger Delta oilfields. The feedforward backpropagation (FFBP) neural networks were trained based on maximum-minimum and clip normalization methods using the Levenberg-Marquardt learning algorithm. With a trial-and-error approach, the architectures that give good performance for the 3-input, 5-input, and 6-input variables network were [3-5-1], [5-6-1], and [6-8-1], respectively. The simplified neural-based models' predictions and their generalization performance were compared with some existing correlations to assess the efficiency of the developed models. From the performances of the simplified neural-based models, the under-listed conclusions are visible:

1) the simplified 3-input-based neural models predicted that the oil flow rate was close to the field flow rate with overall MSE and R values of 9.6185×10^{-4} and 0.9843 for maximum-minimum normalization approach and 5.7986×10^{-3} and 0.9830 for the clip scaling method;
2) the 5-input-based neural models predicted oil flow rate had overall MSE and R values of 5.7790×10^{-4} and 0.9932 for the maximum-minimum normalization approach and 3.7243×10^{-3} and 0.9859 for the clip scaling method;
3) also, the 6-input-based neural models had overall MSE and R values of 8.7520×10^{-4} and 0.9904 for the maximum-minimum normalization approach and 3.8859×10^{-3} and 0.9895 for the clip scaling method;
4) the relative importance (RI) of the neural-based models' input variables on oil flow rate is normalization (i.e., scaling) approach dependent, and the overall RI ranking of the input parameters for oil flow rate prediction is $S>GLR>P_{wh}>T/T_{sc}>\gamma_o>BS\&W>\gamma_g$;
5) when compared with some empirical correlations, the neural-based models predicted oil flow rate resulted in the highest R^2 and lowest RMSE, ARE and AARE values than the existing empirical correlations;
6) the generalization performance of the simplified neural-based models, 3-input-based and 6-input-based with the test datasets resulted in R^2, RMSE, ARE, and AAPRE of 0.9820, 205.78, 0.0248 and 0.1275, respectively, for 3-input-based neural model and R^2 of 0.9264, RMSE of 2089.93, ARE of 0.1656 and AARE of 0.2267 for the 6-input-based neural model; and
7) finally, the generalization performance of the simplified neural-based models was outstanding and comparable with the test datasets to some existing empirical correlations.

Abbreviations

AARE	Average Absolute Relative Error
AI	Artificial Intelligence
ANN	Artificial Neural Network
ANN-CS	Clip Scaling Trained ANN
ANN-MS	Maximum-Minimum Scaling trained ANN
ARE	Average Relative Error
A_t	Tubing Cross-Section Area
BHP	Bottomhole Pressure
BHT	Bottomhole Temperature
BS&W	Basic Sediment & Water
CF	Contribution Factor
CNN	Convolution Neural Network
DNN	Deep Neural Network
Coef. of Var.	Coefficient of Variance
D_{OH}	Open Hole Size
FBHP	Flowing Bottomhole Pressure
FFBP	Feed-Forward Back-Propagation
GLR	Gas-Liquid Ratio
GOR	Gas-Oil Ratio
H	Well Depth
H-test	Kruskal-Wallis Test
k	Permeability
Kurt.	Kurtosis
L_e	Effective Length
MAPE	Mean Absolute Percentage Error
MISO	Multiple-Inputs Single-Output

ML	Machine Learning
MLP	Multilayer Perceptron
MSE	Mean Square Error
n_L	Number of Laterals
P_{fl}	Flowline Pressure
P_{gl}	Gas lift Pressure
P_R	Reservoir Pressure
P_{wh}	Wellhead Pressure
q_{cL}	Critical Liquid flow Rate
q_{gl}	Gas Lift Rate
q_L	Liquid Flow Rate
q_o	Oil Flow Rate
q_{oc}	Critical Oil flow Rate
R	Correlation Coefficient
R^2	Coefficient of Determination
RF	Random Forest
RBF	Radial Basis Function
RI	Relative Importance
RMSE	Root Mean Square Error
RNN	Recurrent Neural Network
S	Choke (Bean) Size
T	Temperature
THP	Tubing Head Pressure
T_{sc}	Temperature at Surface Condition
WHT	Wellhead Temperature
WCT	Water-Cut
χ^2	Chi-Square
γ_g	Gas Gravity
γ_o	Oil Gravity

Funding

The funding for this research was provided by Tertiary Education Trust Fund (TETFund) Nigeria under the National Research Fund. Grant Number: TETF/ES/DR&D-CE/NRF2021/SETI/GEO/00104/01/VOL.1.

Data Availability Statement

The Niger Delta datasets used in the study are available upon request and approval from the Nigerian Upstream Petroleum Regulatory Commission (NUPRC). The Iran Oilfields datasets used for the models' generalization evaluation are available at https://doi.org/10.1016/j.fuel.2017.06.131.

Conflicts of Interest

The authors declare no conflicts of interest.

References

[1] Bikmukhametov T, Jäschke J (2020) First principles and machine learning virtual flow metering: A literature review. J Pet Sci Eng, 184: 106487-106592. https://doi.org/10.1016/j.petrol.2019.106487

[2] Al-Jawad MS, Ottba DJS (2006) Well performance analysis based on flow calculations and IPR. J Eng, 13(3): 822-841. https://doi.org/10.31026/j.eng.2006.03.28

[3] Agwu OE, Alkouh A, Alatefi S, Azim RA, Ferhadi R (2024) Utilization of machine learning for the estimation of production rates in wells operated by electrical submersible pumps. J Pet Explor Prod Technol, 14: 1205–1233. https://doi.org/10.1007/s13202-024-01761-3

[4] Beiranvand MS, Mohammadmoradi P, Aminshahidy B, Fazelabdolabadi B, Aghahoseini S (2012) New multiphase choke correlations for a high flow rate Iranian Oil Field. J Mech Sci, 3: 43-47. https://doi.org/10.5194/ms-3-43-2012

[5] Okon AN, Appah D (2018) Water coning prediction: An evaluation of horizontal well correlations. Eng and Applied Sci J, 3(1): 21-28. https://doi.org/10.11648/j.eas.2018301.14

[6] Ejoh E (2017) How Nigeria 'lost N2 trillion to poor metering of oil wells' in two years. Vanguard Online. https://www.vanguardngr.com/2017/05/nigeria-lost-n2-trillion-poor-metering-oil-wells-two-years/

[7] Brill JP (2010) Modeling multiphase flow in pipes. Soc Pet Eng.: The Way Ahead, 6(2): 16-17.

[8] Lak A, Azin R, Osfouri S, Fatehi R (2017) Modelling critical flow through choke for a gas-condensate reservoir based on drill stem test data. Iranian J Oil & Gas Sci and Technol, 6(3): 29-40. https://doi.org/10.22050/ijogst.2017.69063.1371

[9] Nasriani HR, Kalantariasl A (2011) Two-phase flow choke performance in high-rate gas condensate wells. Paper presented at the Society of Petroleum Engineers Asia Pacific Oil and Gas Conference and Exhibition, Jakarta, Indonesia, 20-22 Sept. 2011. https://doi.org/10.2118/145576-MS

[10] Hong KC, Griston S (1997) Best practice for the distribution and metering of two-phase steam. Soc Pet Eng. Production Facility, 12(3): 173-80. https://doi.org/10.2118/35422-PA

[11] Sadatshojaei E, Jamialahmadi M, Esmaeilzadeh F, Ghazanfari MH (2016) Effects of low-salinity water coupled with silica nanoparticles on wettability alteration of dolomite at reservoir temperature. J Pet Sci Technol, 34(15): 1345-1351. https://doi.org/10.1080/10916466.2016.1204316

[12] Choubineh A, Ghorbani H, Wood DA, Moosavi SR, Khalafi E, Sadatshojaei E (2017) Improved predictions of wellhead choke liquid critical-flow rates: Modelling based on hybrid neural network training learning-based optimization. Fuel, 207: 547-560. https://doi.org/10.1016/j.fuel.2017.06.131

[13] Al-Attar HH (2009) New correlations for critical and subcritical two-phase flow through surface chokes in high-rate oil wells. Paper presented at the Latin American and Caribbean Petroleum Engineering Conference, Cartagena de Indias, Colombia, 31 May-30 June 2009. https://doi.org/10.2118/120788-MS

[14] Gilbert WE (1954) *Flowing and gas-lift well performance*. American Petroleum Institute Drilling & Production Practice, Dallas, Texas, 20: 126-157.

[15] Baxendell PB (1957) Bean Performance-Lake Wells. Shell Internal Report, October 1957.

[16] Ros NCJ (1960) An analysis of critical simultaneous gas/liquid flow through a restriction and its application to flow metering. Applied Sci Res, 9: 374-389. https://doi.org/10.1007/BF00382215

[17] Achong I (1961) Revised bean performance formula for Lake Maracaibo wells. Shell Internal Report, Oct. 1961.

[18] Omana R, Houssier C, Brown KE, Brill JP, Thompson RE (1968) Multiphase flow through chokes. Paper presented at the Society of Petroleum Engineers Annual Meeting, Denver Colorado, 28 Sept. - 1 Oct. 1968. https://doi.org/10.2118/2682-MS

[19] Pilehvari AA (1981) Experimental study of critical two-phase flow through wellhead chokes. University of Tulsa Fluid Flow Project Report, Tulsa, USA.

[20] Owolabi OO, Dune KK, Ajienka JA (1991) Producing the multiphase flow performance through wellhead chokes for the Niger Delta oil wells. Paper presented at the International Conference of the Society of Petroleum Engineers Nigeria Section Annual Proceeding, August 1991.

[21] Al-Towailib A, Al-Marhoun MA (1994) A new correlation for two-phase flow through chokes. J Can Pet Technol, 33(5): 40-43. https://doi.org/10.2118/94-05-03

[22] Khorzoughi MB, Beiranvand M, Rasaei MR (2013) Investigation of a new multiphase flow choke correlation by linear and non-linear optimization methods and Monte Carlo sampling. J Pet Explor Prod Technol, 3: 279-285. https://doi.org/10.1007/s13202-103-0067-9

[23] Okon AN, Udoh FD, Appah D (2015) Empirical wellhead pressure production rate correlations for Niger Delta oil wells. Paper presented at the Society of Petroleum Engineers (SPE), Nigeria Council 39th Nigeria Annual International Conference and Exhibition, Eko Hotel and Suite, Lagos, 4-6 Aug. 2015. http://dx.doi.org/10.2118/178303-MS

[24] Ghorbani H, Wood DA, Choubineh A, Tatar A, Abarghoy PG, Madani M, Mohamadian N (2018) Prediction of oil flow rate through an orifice flow meter: artificial intelligence alternatives compared. Petroleum 6 (4): 404-414. https://doi.org/10.1016/j.petlm.2018.09.003

[25] Alrumah M, Alenezi RA (2019) New universal two-phase choke correlations developed using non-linear multivariable optimization technique. J Eng Res, 7(3): 320-329.

[26] Joshua SK, Oshokosikeshishi LP, Sylvester O (2020) New production rate model of wellhead choke for Niger Delta oil wells. J Pet Sci Tech, 10: 41-49. https://doi.org/10.22078/jpst.2020.3925.1630

[27] Alarifi SA (2022). Workflow to predict wellhead choke performance during multiphase flow using machine learning. J Pet Sci Eng, 214 (2022)110563. https://doi.org/10.1016/j.petrol.2022.110563

[28] Berneti SM, Shahbazian M (2011) An imperialist competitive algorithm artificial neural network method to predict oil flow rate of the wells. Int. J. Comput. Appl. 26(10): 47-50.

[29] Mirzaei-Paiaman A, Salavati S (2012) The application of artificial neural networks for the prediction of oil production flow rate. Energy Sources, Part A: Recovery, Utilization, and Environmental Effects, 34(19): 1834-1843. http://doi.org/10.1080/15567036.2010.492386

[30] Al-Khalifa MA, Al-Marhoun MA (2013) Application of neural network for two-phase flow through chokes. Paper presented at the Society of Petroleum Engineers Saudi Arabia section Annual Technical Symposium and Exhibition, Khobar, Saudi Arabia, 19-22 May 2013. https://doi.org/10.2118/169597-MS

[31] Zangl G, Hermann R, Schweiger C (2014) Comparison of methods for stochastic multiphase flow rate estimation. Paper presented at the Society of Petroleum Engineers Annual Technical Conference and Exhibition, Amsterdam, The Netherlands, 27-29 Oct. 2014. https://doi.org/10.2118/170866-MS

[32] Al-Ajmi MD, Alarifi SA, Mahsoon AH (2015) Improving multiphase choke performance prediction and well production test validation using artificial intelligence: A new milestone. Paper presented at the Society of Petroleum Engineers Digital Energy Conference and Exhibition, Woodlands, Texas, USA, 3-5 Mar. 2015. https://doi.org/SPE-173394-MS

[33] Okon AN, Appah D (2016) Neural network models for predicting wellhead pressure-flow rate relationship for Niger Delta oil wells. J Scientific Res Reports, 12(1): 1-14. https://doi.org/10.9734/JSRR/2016/28715

[34] Al-Qutami TA, Ibrahim R, Ismail I, Ishak MA (2018) Virtual multiphase flow metering using diverse neural network ensemble and adaptive simulated annealing. Expert Syst. Appl. 93(1): 72-85. https://doi.org/10.1016/j.eswa.2017.10.014

[35] Al-Kadem M, Al Dabbous M, Al Mashhad A, Al Sadah H (2019) Utilization of artificial neural networking for real-time oil production rate estimation. Paper presented at the Abu Dhabi International Petroleum Exhibition and Conference, Abu Dhabi, UAE, 11-14 Nov. 2019. https://doi.org/10.2118/197879-MS

[36] Khan MR, Tariq Z, Abdulraheem A (2020) Application of artificial intelligence to estimate oil flow rate in gas-lift wells. Natural Resources Research, 29: 4017-4029. https://doi.org/10.1007/s11053-020-09675-7

[37] Ibrahim NM, Alharbi AA, Alzahrani TA, Abdulkarim AM, Alessa IA, Hameed AM, Albabtain AS, Alqahtani DA, Alsawwaf MK, Almuqhim AA (2022) Well performance classification and prediction: deep learning and machine learning long term regression experiments on oil, gas, and water production. Sensors, 22, 5326. https://doi.org/10.3390/s22145326

[38] Okorugbo O, Dune KK, Wami EN (2021) Application of neural network-particle swarm modelling for predicting wellhead choke performance in the Niger Delta. Int J Pet Petrochem Eng, 7(1): 21-29. https://doi.org/10.20431/2454-7980.0701003

[39] Park YS, Lek S (2016) Artificial neural networks: multilayer perceptron for ecological modelling. In S. E. Jørgensen (Ed.), *Developments in environmental modelling*, 28: 123-140). Elsevier. https://doi.org/10.1016/B978-0-444-63623-2-00007-4

[40] Behnoud P, Hosseini P (2017) Estimation of lost circulation amount occurs during under balanced drilling using drilling data and neural network. Egyptian J Pet, 26(3): 627-634. https://doi.org/10.1016/j.ejpe.2016.09.004

[41] Mekanik F, Imteaz M, Gato-Trinidad S, Elmahdi A (2013) Multiple regression and artificial neural network for long term rainfall forecasting using large scale climate modes. J. Hydrol, 503(2): 11-21. https://doi.org/10.1016/j.jhydrol.2013.08.035

[42] Demuth, H., Beale, M., Martin, H. (2009). Neural network toolbox users guide. The Mathworks, Inc, p. 906, Version 6.

[43] Haykin S (1999) *Neural networks, a comprehensive foundation*, Second ed. Prentice Hall Inc., Upper Saddle River.

[44] Aalst WMP, Rubin V, Verbeek HMW, Van Dongen BF, Kindler E, Günther CW (2010) Process mining: a two-step approach to balance between underfitting and overfitting. Software Syst. Model, 9(1): 87-111. https://doi.org/10.1007/s10270-008-0106-z

[45] Anifowose F, Ewenla A, Eludiora S (2012) Prediction of oil and gas reservoir properties using support vector machines. Paper presented at the International Petroleum Technical Conference, Bangkok, Thailand, 7-9 Feb. 2012. https://doi.org/10.2523/IPTC-14514-MS

[46] Okon AN, Ansa IB (2021) Artificial neural network models for reservoir aquifer dimensionless variables: influx and pressure prediction for water influx calculation. J Pet Explor Prod Technol, 11(4): 1885-1904. https://doi.org/10.1007/s13202-021-01148-8

[47] Perkins TK (1993) Critical and subcritical flow of multiphase mixtures through chokes. Society of Petroleum Engineering Drilling and Completion, 8(4): 271-276. https://doi.org/10.2118/20633-PA

[48] Ibrahim AF, Al-Dhaif R, Elkatatny S, Al Shehri D (2021) Applications of artificial intelligence to predict oil rate for high gas-oil ratio and water-cut wells. ACS Omega, 6: 19484-19493. https://doi.org/10.1021/acsomega.1c01676

[49] Barjouei HS, Ghorbani H, Mohamadian N, Wood DA, Davoodi S, Moghadasi J, Saberi H (2021) Prediction performance advantages of deep machine learning algorithms for two‐phase flow rates through wellhead chokes. J Pet Explor Prod, 11: 1233–1261. https://doi.org/10.1007/s13202-021-01087-4

[50] Ahmadi MA, Ebadi M, Shokrollahi A, Majidic SMJ (2013) Evolving artificial neural network and imperialist competitive algorithm for prediction oil flow rate of the reservoir. Appl. Soft Comput. 13 (2), 1085-1098. https://doi.org/10.1016/j.asoc.2012.10.009

[51] Gorjaei RG, Songolzadeh R, Torkaman M, Safari M, Zargar G (2015) A novel PSO-LSSVM model for predicting liquid rate of two-phase flow through wellhead chokes. J Nat Gas Sci Eng, 24: 228-237.

[52] Hasanvand M, Berneti SM (2015) Predicting oil flow rate due to multiphase flow meter by using an artificial neural network. Energy Sources, Part A: Recovery, Utilization, and Environmental Effects, 37(8): 840-845. https://doi.org/10.1080/15567036.2011.590865

[53] Baghban A, Abbasi P, Rostami P, Bahadori M, Ahmad Z, Kashiwao T, Bahadori A (2016) Estimation of oil and gas properties in petroleum production and processing operations using rigorous model. J Pet Sci Tech, 34(13): 1129-1136. https://doi.org/10.1080/10916466.2016.1183028

[54] Buhulaigah A, Al-Mashhad AS, Al-Arifi SA, Al-Kadem MS, Al-Dabbous MS (2017) Multilateral wells evaluation utilizing artificial intelligence. Paper presented at the Society of Petroleum Engineers Middle East Oil & Gas Show and Conference, Manama, Kingdom of Bahrain, 6-9 Mar. 2017. https://doi.org/10.2118/183688-MS

[55] Khan MR, Alnuaim S, Tari Z, Abdulraheem A (2019) Machine learning application for oil rate prediction in artificial gas lift wells. Paper presented at the Society of Petroleum Engineers Middle East Oil and Gas Show and Conference, Manama, Bahrain, 18-21 Mar. 2019. https://doi.org/10.2118/194713-MS

[56] Ghorbani H, Wood, DA, Moghadasi J, Choubineh A, Abdizadeh P, Mohamadian, N (2019) Predicting liquid flow-rate performance through wellhead chokes with genetic and solver optimizers: an oil field case study. J Pet Explor Prod Technol, 9: 1355-1373. https://doi.org/10.1007/s13202-018-0532-6

[57] Al-Rumah M, Aladwani F, Alatefi S (2020) Toward the development of a universal choke correlation - global optimization and rigorous computational techniques. J Eng Res, 8(3): 240-254. https://doi.org/10.36909/jer.v8i3.7717

[58] Marfo SA, Kporxah C (2020) Predicting oil production rate using artificial neural network and decline curve analytical methods. Proceedings of 6th UMaT Biennial International Mining and Mineral Conference, Tarkwa, Ghana, 43-50.

[59] Azim RA (2022) A new correlation for calculating wellhead oil flow rate using artificial neural network. J Artificial Intelligence in Geosciences, 3: 1-7. https://doi.org/10.1016/j.aiig.2022.04.001

[60] Okon AN, Effiong AJ, Daniel DD (2023) Explicit neural network-based models for bubble point pressure and oil formation volume factor prediction. Arabian J Sci Eng, 48: 9221-9257. https://doi.org/10.1007/s13369-022-07240-3

[61] Mahmoudi S, Mahmoudi A (2014) Water saturation and porosity prediction using back-propagation artificial neural network (BPANN) from well log data. J Eng & Technol 5(2): 1-8. https://jet.utem.edu.my/jet/article/view/153

[62] Okon AN, Adewole SE, Uguma EM (2020) Artificial neural network model for reservoir petrophysical properties: porosity, permeability and water saturation prediction. J Model Earth Syst and Environ, 7: 2373-2390. https://doi.org/10.1007/s40808-020-01012-4

[63] Abuh FA, Akpabio JU, Okon AN (2023) Machine learning-based models for basic sediment & water and sand-cut prediction in matured Niger Delta fields. J Energy Res Reviews 15(2): 70-93. https://doi.org/10.9734/jenrr/2023/v15i2310

[64] Al-Bulushi N, King PR, Blunt MJ, Kraaijveld M (2009) Development of artificial neural network models for predicting water saturation and fluid distribution. J Pet Sci Eng 68: 197-208. https://doi.org/10.1016/j.petrol.2009.06.017

[65] Sircar A, Yadav K, Rayavarapu K, Bist N, Oza H (2021) Application of machine learning and artificial intelligence in oil and industry. Pet Res, 6: 379-391. https://doi.org/10.1016/j.ptlrs.2021.05.009

[66] Effiong AJ, Etim JO, Okon AN (2021) Artificial intelligence model for predicting formation damage in oil and gas wells. Paper presented at the Society of Petroleum Engineers (SPE), Nigeria Council 45th Nigeria Annual International Conference and Exhibition, 2-4 Aug. 2021. http://dx.doi.org/10.2118/207129-MS

[67] George A (2021) Predicting oil production flow rate using artificial neural networks – the Volve field case. Paper presented at the Nigeria Annual International Conference and Exhibition, Logas, Nigeria, 2-4 August 2021. https://doi.org/10.2118/208258-MS

[68] Citakoglu H, Coskun O (2022) Comparison of hybrid machine learning methods for the prediction of short-term meteorological droughts of Sakarga Meterological Station in Turkey. Environ Sci Poll Res. https://doi.org/10.1007/s11356-022-21083-3

[69] Demir V (2022) Enhancing monthly lake levels forecasting using heuristic regression techniques with periodicity data component: application of Lake Michigan. Theor Appl Climatol 148: 915-929. https://doi.org/10.1007/s00704-022-03982-0

[70] Alexander D, Tropsha A, Winkler D (2015) Beware of R^2: simple, unambiguous assessment of the prediction accuracy of QSAR and QSPR Models. J Chem Info Model, 55(7): 1316-1322. https://doi.org/10.1021/acs.jcim.5b00206